The Plant Cell, Vol. 24: 5089–5105, December 2012, www.plantcell.org © 2012 American Society of Plant Biologists. All rights reserved.

The R2R3-MYB–Like Regulatory Factor EOBI, Acting Downstream of EOBII, Regulates Scent Production by Activating *ODO1* and Structural Scent-Related Genes in Petunia[C][W]

Ben Spitzer-Rimon, Moran Farhi, Boaz Albo, Alon Cna'ani, Michal Moyal Ben Zvi, Tania Masci, Orit Edelbaum, Yixun Yu, Elena Shklarman, Marianna Ovadis, and Alexander Vainstein[1]

The Robert H. Smith Institute of Plant Sciences and Genetics in Agriculture, The Hebrew University of Jerusalem, Rehovot 76100, Israel

Flower scent is a highly dynamic trait, under developmental, spatial, and diurnal regulation. The mechanism governing scent production is only beginning to be unraveled. In petunia (*Petunia hybrida*), EMISSION OF BENZENOIDS II (EOBII) controls transcription of both the shikimate pathway-regulating MYB factor *ODORANT1* (*ODO1*) and phenylpropanoid scent-related structural genes. A promoter-activation screen identified an R2R3-MYB–like regulatory factor of phenylpropanoid volatile biosynthesis acting downstream of EOBII, designated *EOBI*. *EOBI* silencing led to downregulation of *ODO1* and numerous structural scent-related genes from both the shikimate and phenylpropanoid pathways. The ability of EOBI to directly activate *ODO1*, as revealed by electrophoretic mobility shift assay and yeast one-hybrid analysis, place EOBI upstream of ODO1 in regulating substrate availability for volatile biosynthesis. Interestingly, *ODO1*-silenced transgenic petunia flowers accumulated higher *EOBI* transcript levels than controls, suggesting a complex feedback loop between these regulatory factors. The accumulation pattern of *EOBI* transcript relative to *EOBII* and *ODO1*, and the effect of up/downregulation of *EOBII* on transcript levels of *EOBI* and *ODO1*, further support these factors' hierarchical relationships. The dependence of scent production on *EOBI* expression and its direct interaction with both regulatory and structural genes provide evidence for *EOBI*'s wide-ranging involvement in the production of floral volatiles.

INTRODUCTION

Floral scent is a complex trait determined by a combination of low molecular weight compounds (Knudsen et al., 2006; Colquhoun and Clark, 2011). These molecules serve as an airborne signal mediating plant–plant and plant–insect interactions, thereby impacting plant reproduction and fitness (Hoballah et al., 2005; Horiuchi et al., 2007; Goodrich and Raguso, 2009; Klahre et al., 2011; Pichersky and Lewinsohn, 2011). Plant volatiles are biosynthesized mainly through the terpenoid, fatty acid, and phenylpropanoid pathways (Croteau and Karp, 1991; Dudareva et al., 2004). Phe, the precursor of phenylpropanoid compounds, is biosynthesized via the shikimate pathway, which was recently shown to operate mainly through the arogenate route in planta (Maeda et al., 2010, 2011; Vogt, 2010; Dal Cin et al., 2011). Phe is converted through the action of L-Phe ammonia lyase (PAL) and subsequent enzymatic reaction into a vast array of volatile compounds (Dudareva et al., 2004; Guterman et al., 2006; Dexter et al., 2007; Koeduka et al., 2008; Hippauf et al., 2010; Vogt, 2010). Volatile phenylpropanoids include, among others, eugenol, isoeugenol, and vanillin, as well as C6-C1 benzenoids, such as benzaldehyde, benzyl alcohol, and methylbenzoate (Boatright et al., 2004; Long et al., 2009; Van Moerkercke et al., 2009). Another group of volatile phenylpropanoids derive from Phe via the action of phenylacetaldehyde synthase, resulting in phenylacetaldehyde and downstream volatiles (Kaminaga et al., 2006; Tieman et al., 2006; Farhi et al., 2010).

The role of transcriptional regulation in reprogramming metabolic processes during plant development and in response to biotic and abiotic cues has been recognized in several plant systems. Nevertheless, our limited knowledge of regulatory networks governing secondary metabolism, including that of scent production, comes mainly from studies on flavonoid biosynthesis (Koes et al., 2005; Schwinn et al., 2006; Schwachtje and Baldwin, 2008; Aharoni and Galili, 2011; Feller et al., 2011). In addition, involvement of transcriptional regulators in the biosynthesis of alkaloids, mainly in response to jasmonate (van der Fits and Memelink, 2000) and glucosinolates (Malitsky et al., 2008; Burow et al., 2010; Sønderby et al., 2010), was recently revealed. Despite the long concerted effort into studying carotenoid biosynthesis, one of the most important classes of plant metabolites, only one direct transcriptional regulator of the pathway has been revealed to date (Toledo-Ortiz et al., 2010).

The first regulator of scent production, *ODORANT1* (*ODO1*), was identified using a genomic/transcriptomic approach. ODO1 was shown to regulate transcript levels of genes encoding

[1] Address correspondence to vain@agri.huji.ac.il.
The author responsible for distribution of materials integral to the findings presented in this article in accordance with the policy described in the Instructions for Authors (www.plantcell.org) is: Alexander Vainstein (vain@agri.huji.ac.il).
[C] Some figures in this article are displayed in color online but in black and white in the print edition.
[W] Online version contains Web-only data.
www.plantcell.org/cgi/doi/10.1105/tpc.112.105247

shikimate pathway enzymes that, in turn, affected metabolic flow toward phenylpropanoid production (Verdonk et al., 2005). The importance of regulating flux toward phenylpropanoids was also demonstrated in petunia (*Petunia hybrida*) flowers overexpressing the *Arabidopsis thaliana* MYB factor *PRODUCTION OF ANTHOCYANIN PIGMENT1* (*PAP1*) (Ben Zvi et al., 2008). Recently, MYB factor Ph MYB4, which suppresses production of *p*-coumaric acid–derived volatiles, such as eugenol and isoeugenol, through downregulation of genes encoding upstream cinnamate 4-hydroxylase, was identified (Colquhoun et al., 2011a). EMISSION OF BENZENOIDS II (EOBII), similar to PAP1 and in contrast with ODO1, has been shown to regulate the transcription of both shikimate pathway genes and genes directly involved in the biosynthesis of phenylpropanoid volatiles (Verdonk et al., 2005; Dare et al., 2008; Ben Zvi et al., 2008; Spitzer-Rimon et al., 2010; Zvi et al., 2012). While it has been recently suggested that EOBII may also have activities outside the scope of floral scent production (Colquhoun et al., 2011b), the epistatic relations between EOBII and ODO1 have been confirmed: EOBII binds directly to ODO1's upstream regulatory sequence and transcriptionally activates its expression (Van Moerkercke et al., 2011).

In this article, using EOBII as the hound in a promoter-activation screen, we identified a downstream partner, designated EOBI, which regulates floral scent by directly modulating the expression of both *ODO1* and phenylpropanoid structural scent-related genes. A model describing regulation of floral scent production based on the hierarchical interrelationship between petunia regulatory factors and their downstream targets is presented.

RESULTS

Identification of Scent-Related Factor EOBI by Promoter-Activation Screen in *EOBII*-Expressing Protoplasts

We tested the relevance to floral scent production of a collection of putative regulatory factors isolated from petunia flowers using the virus-induced gene silencing system. In addition to the previously characterized *EOBII*, several candidates that affected floral scent emission were identified. Whereas suppression of *EOBI* led to decreased floral scent production, downregulation of *EOBIII* and *EOBV* led to increases in the levels of emitted volatiles (see Supplemental Figure 1 online). To identify putative scent-related regulatory factors affected by EOBII, we employed a protoplast-based system: We coinfected protoplasts expressing EOBII with promoter sequences of candidate scent-related factors fused to autofluorescent reporter genes. *Discosoma* sp fluorescent protein (DsRed) signal, indicative of promoter activation by EOBII, was generated in protoplasts cotransformed with the promoter region of the sequence termed EOBI fused to DsRed ($EOBI_{pro}$:DsRed) and *EOBII* under the control of the 35S promoter ($35S_{pro}$:EOBII) (Figures 1Aa to 1Ac). Control protoplasts cotransformed with unrelated MYB factor MYBYS driven by the 35S promoter ($35S_{pro}$:MYBYS; Leitner-Dagan et al., 2006) or cyan fluorescent protein (CFP; $35S_{pro}$:CFP) instead of $35S_{pro}$:EOBII and $EOBI_{pro}$:DsRed did not yield DsRed fluorescent signal (Figures 1Ag to 1Al). The ability of EOBI to activate the *EOBII* promoter was also tested: No DsRed fluorescence was detected in

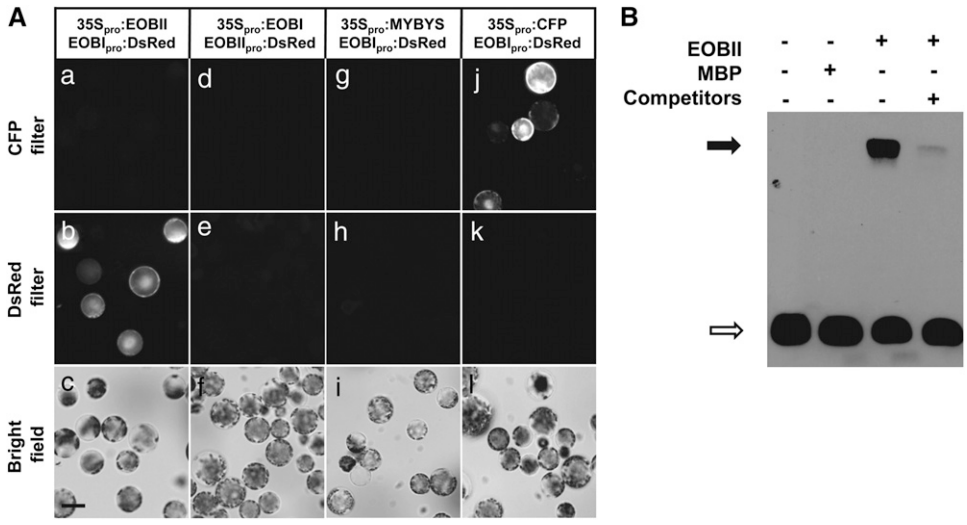

Figure 1. EOBII Interacts with the *EOBI* Promoter.

(A) Petunia protoplasts were cotransformed with 35S-driven *EOBII* ($35S_{pro}$:EOBII) and DsRed driven by the petunia *EOBI* promoter ($EOBI_{pro}$:DsRed) (**[a]** to **[c]**) or with 35S-driven *EOBI* ($35S_{pro}$:EOBI) and DsRed driven by the petunia *EOBII* promoter ($EOBII_{pro}$:DsRed) (**[d]** to **[f]**). As controls, protoplasts were cotransformed with $EOBI_{pro}$:DsRed and cucumber (*Cucumis sativus*) *MYBYS* driven by the 35S promoter ($35S_{pro}$:MYBYS) (**[g]** to **[i]**) or $35S_{pro}$:CFP (**[j]** to **[l]**). CFP, DsRed, and bright-field images are shown in the top (**[a]**, **[d]**, **[g]**, and **[j]**), middle (**[b]**, **[e]**, **[h]**, and **[k]**), and bottom (**[c]**, **[f]**, **[i]**, and **[l]**) panels, respectively. Bar = 50 μm.

(B) EMSA of *EOBI* promoter fragment in the presence of EOBII. Biotinylated *EOBI* promoter fragment containing the putative MYB binding domain (CTAACT; Sablowski et al., 1994) was used as the probe. MBP was used as a control protein. Black arrow indicates protein-DNA complexes. White arrow shows the position of the free probe (bottom left). In the lane with competitor DNA, + indicates 1000× molar excess of nonlabeled probe.

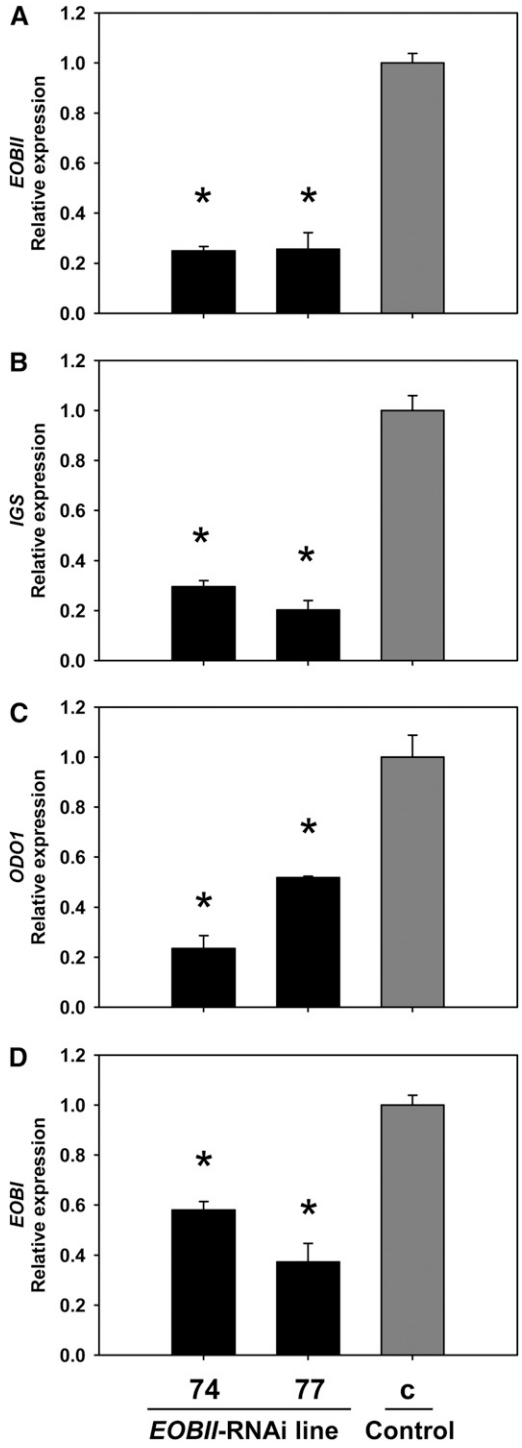

Figure 2. *EOBII* Silencing Results in *EOBI* Downregulation.

Quantitative real-time PCR analysis of *EOBII*, *IGS*, *ODO1*, and *EOBI* transcript levels in two independent lines (74 and 77) of EOBII-RNAi–silenced petunia corollas 1 d after anthesis compared with control $35S_{pro}$:GUS transgenic corollas (c). Presented data (three biological replicates, each consisting of three technical repeats) were normalized to those from control corollas with SE indicated by vertical lines. Significance of differences ($P \leq 0.05$) between treatments and control (asterisks) were calculated using Dunnett's method following analysis of variance (ANOVA) based on the raw transcript levels' data normalized to *Actin*.

protoplasts cotransformed with *EOBI* driven by the 35S promoter ($35S_{pro}$:EOBI) and the DsRed gene driven by the EOBII promoter (EOBIIpro:DsRed) (Figures 1Ad to 1Af). Overexpression of EOBII in flowers infiltrated with *Agrobacterium tumefaciens* carrying $35S_{pro}$:EOBII also led to increased levels of *EOBI* transcript (see Supplemental Figure 2 online), further establishing the capacity of EOBII to activate *EOBI* expression.

EOBI promoter contains a potential consensus MYB binding sequence (CTAACT; Sablowski et al., 1994) 1193 nucleotides upstream of the transcriptional start point. To assay the interaction between EOBII and *EOBI* promoter, an electrophoretic mobility shift assay (EMSA) was employed using the candidate MYB binding sequence as the probe. To analyze formation of protein-DNA complex, EOBII recombinant protein (fused to maltose binding protein [MBP]) was incubated with a labeled *EOBI* promoter fragment with or without competitor DNA. Gel shift assays (Figure 1B) showed that EOBII recombinant protein can interact with the *EOBI* promoter. The unlabeled *EOBI* promoter fragment was able to compete with the labeled *EOBI* fragment for EOBII binding, and the mobility shift was not seen in control reactions lacking EOBII, indicating a specific interaction between EOBII and *EOBI* promoter.

To further establish the interplay between EOBI and EOBII, petunia (W115) transgenic lines with RNA interference (RNAi)–suppressed *EOBII* were generated and the effect of *EOBII* suppression on the expression levels of *EOBI* and other floral scent-related genes was examined. *EOBII* transcript levels were reduced by 70 to 80% in flowers of independent EOBII-RNAi transgenic lines 74 and 77 compared with that in control $35S_{pro}$:GUS (for β-glucuronidase) transgenic lines (Figure 2A). As expected based on the results generated using virus-induced gene silencing–suppressed *EOBII* flowers (Spitzer-Rimon et al., 2010), transcript levels of *ISOEUGENOL SYNTHASE* (*IGS*) and *ODO1* were significantly downregulated in these EOBII-RNAi lines (Figures 2B and 2C). *EOBI* transcript also accumulated to lower levels in flowers of these EOBII-RNAi transgenic lines compared with control flowers (Figure 2D).

EOBI Is a Nuclear-Localized Flower-Specific R2R3-MYB Factor

EOBI expression was analyzed in various organs of petunia, in flowers at different stages of development, and at various time points during the day and night by real-time RT-PCR (Figure 3). *EOBI* expression was detected exclusively in flower organs, with the highest levels in flower limbs. The transcript was also detected in the pistil and flower tube and to a very low extent in the stamens. Expression of *EOBI* was not detected in the sepals or in any vegetative tissue (e.g., roots, stems, or leaves) (Figure 3A). The level of *EOBI* transcript in the limbs increased with flower development, reaching maximal levels at anthesis (Figure 3B). The diurnal expression pattern of *EOBI* in the limbs, monitored for three consecutive days following anthesis, was found to be

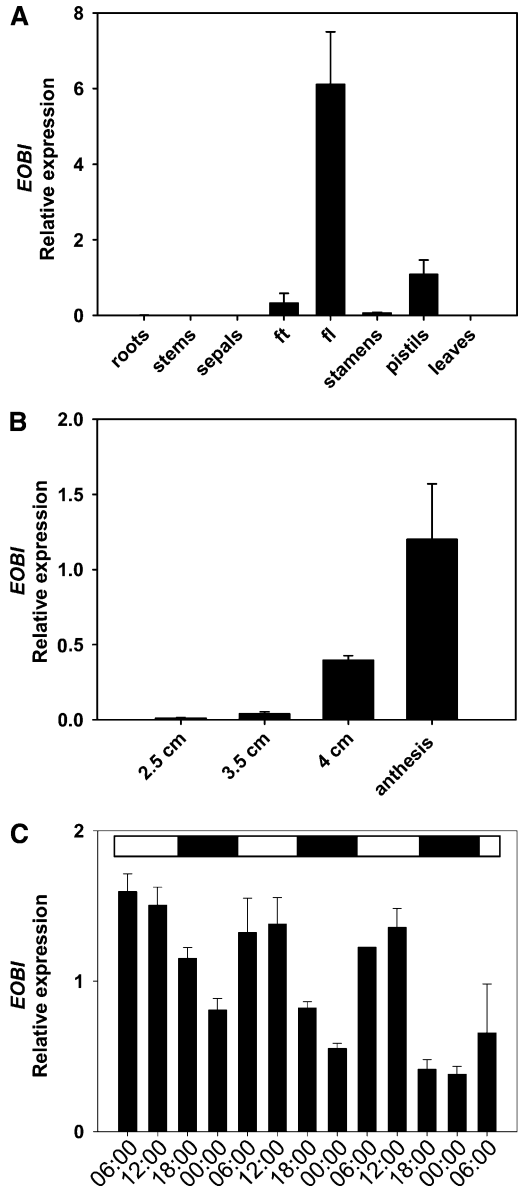

Figure 3. Spatial, Developmental, and Temporal Regulation of *EOBI* Transcript Levels.

Petunia line P720 RNA was extracted from different organs **(A)**, corollas at different developmental stages **(B)**, and corollas at different time points during the day/night **(C)** for three consecutive days (starting at anthesis at 06:00). *EOBI* transcript levels were determined by quantitative real-time PCR analysis using *Actin* as the reference. Graphs represent the average of three to five biological replicates (each consisting of three technical repeats) with SE indicated by vertical lines. Black part of horizontal bar in **(C)** indicates nighttime hours. fl, flower limb; ft, flower tube.

rhythmic, with transcript reaching its highest levels during the day (Figure 3C).

To establish the pattern of *EOBI* promoter activity, we co-infiltrated petunia leaves and flowers (buds and mature flowers) with *Agrobacterium* harboring $EOBI_{pro}$:DsRed and $35S_{pro}$:YFP (for yellow fluorescent protein; used as a reference) binary constructs (Figure 4A). Transient expression of EOBI-driven DsRed was detected in petals of both buds and mature flowers (Figures 4Aa to 4Ac and 4Ag to 4Ai) but not in leaves (Figures 4Am to 4Ao). YFP expression driven by 35S was detected, as expected, in all examined tissues (Figures 4Ab, 4Ah, and 4An). The pattern of *EOBI* promoter activity was compared with that of the scent biosynthetic gene *IGS*, whose promoter sequence has been published (Spitzer-Rimon et al., 2010) and, similar to *EOBI*, is affected by EOBII. The spatial pattern of *IGS* promoter activity was identical to that of *EOBI* promoter, as revealed by infiltration of petunia leaves (Figures 4Ap to 4Ar) and flowers (Figures 4Ad to 4Af and 4Aj to 4Al) with *Agrobacterium* harboring IGS_{pro}:DsRed.

EOBI cDNA contains an open reading frame (ORF) with a conserved R2R3 binding domain (important for interaction with promoter elements; Kranz et al., 1998; Dubos et al., 2010) near its N terminus and a W/Y-MDDIW motif (of major importance for transactivation; Li et al., 2006) at its C terminus (Figure 5A). Based on the motifs outside the DNA binding R2R3, EOBI is clustered into subgroup 19 of the R2R3-MYB transcription factors (Figure 5B; Dubos et al., 2010). It shares homology with other subgroup 19 members, such as *Arabidopsis* MYB21, MYB24, pea (*Pisum sativum*) MYB26, petunia EOBII, *Nicotiana langsdorffii* × *Nicotiana sanderae* MYB305, and snapdragon (*Antirrhinum majus*) MYB305, showing highest phylogenetic similarity to the latter (Figure 5B). Members of this subgroup have been shown to be predominantly expressed in their respective flowers and involved in regulation of the phenylpropanoid pathway (Sablowski et al., 1994; Moyano et al., 1996; Uimari and Strommer, 1997; Shin et al., 2002; Li et al., 2006). Members of subgroup 20, which is relatively close to subgroup 19, such as *Arabidopsis* MYB108, MYB62, and MYB2, are involved in regulating hormonal homeostasis and flower development (Devaiah et al., 2009; Mandaokar and Browse, 2009; Guo and Gan, 2011). Petunia ODO1, distant from EOBI, clusters with *Arabidopsis* MYB42 and MYB85, factors that are involved in the regulation of secondary wall biosynthesis. Negative regulators of floral scent production, such as petunia EOBIII (also termed Ph MYB4; Colquhoun et al., 2011a) and EOBV, cluster to subgroup 4 together with MYB4 and MYB32 from *Arabidopsis* and MYB308 and MYB330 from snapdragon, previously characterized as negative regulators of the phenylpropanoid pathway (Tamagnone et al., 1998; Jin et al., 2000; Preston et al., 2004; Feller et al., 2011).

Based on the PSORT II prediction algorithm (Nakai and Horton, 1999), EOBI is located in the cell nucleus. To experimentally establish EOBI's intracellular localization, we transiently expressed an EOBI:GFP (for green fluorescent protein) fusion protein in *Nicotiana benthamiana* leaves and followed its compartmentalization within the cell. Microscopy analysis localized GFP fluorescence to the nucleus (Figures 4Ba to 4Bc), whereas control GFP (not fused to EOBI) accumulated in the cytosol, as expected (Figures 4Bd and 4Be).

EOBI Is Required for the Expression of Structural and Regulatory Genes Involved in Floral Phenylpropanoid Scent Production

To study EOBI's function in more detail, transgenic petunia (W115) plants with suppressed *EOBI* expression were generated. An ~60 to 80% reduction in *EOBI* transcript levels was observed in the

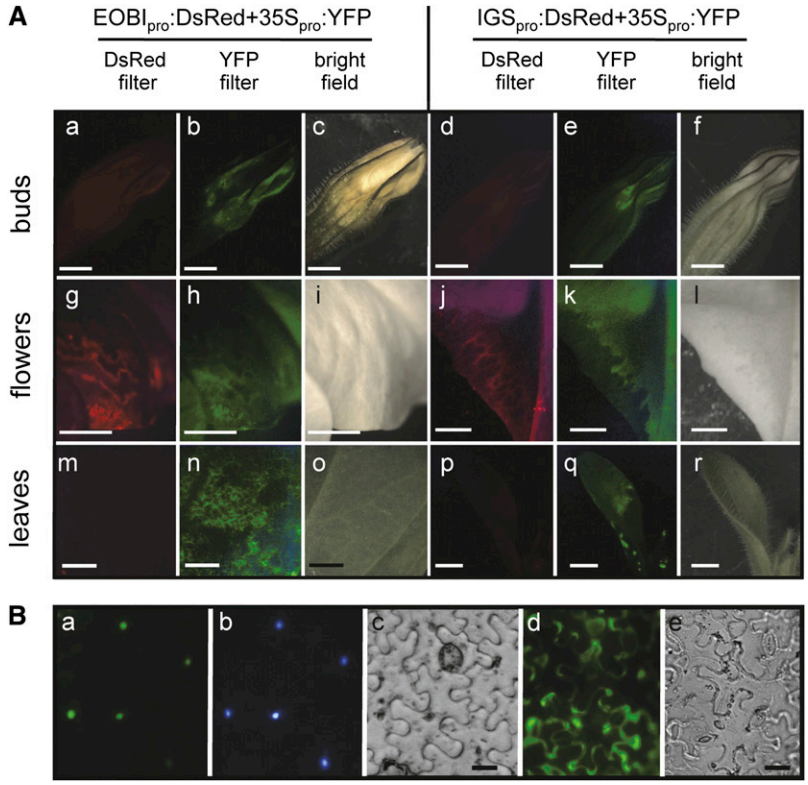

Figure 4. *EOBI* Promoter Activity and Intracellular Localization.

(A) *EOBI* and *IGS* promoter activity in petunia buds (**[a]** to **[f]**), flowers 2 d after anthesis (**[g]** to **[l]**), and leaves (**[m]** to **[r]**) 36 h after infiltration with agrobacteria carrying EOBI$_{pro}$:DsRed or IGS$_{pro}$:DsRed; in both cases, infiltration was performed together with agrobacteria carrying 35S$_{pro}$:YFP as a control. Fluorescence images were analyzed using DsRed filter (**[a]**, **[d]**, **[g]**, **[j]**, **[m]**, and **[p]**), YFP filter (**[b]**, **[e]**, **[h]**, **[k]**, **[n]**, and **[q]**), or bright field (c, f, i, l, o, and r). Bars = 2 mm.

(B) Nuclear localization of EOBI. **(a)** Localization of the EOBI:GFP fusion protein in *N. benthamiana* leaf epidermis; **(b)** nucleus stained with 4′,6-diamidino-2-phenylindole; **(c)** bright field; **(d)** and **(e)** fluorescence of nonfused GFP used as a control and bright field of leaf epidermis, respectively. Bars = 20 μm.

[See online article for color version of this figure.]

three independent transgenic EOBI-RNAi lines compared with the transgenic GUS-expressing control line (Figure 6A; see Supplemental Figure 3 online). Plant development and flower shape and size were similar in EOBI-RNAi and transgenic control lines. The levels of a number of phenylpropanoid volatiles emitted from EOBI-RNAi–suppressed flowers (e.g., benzyl alcohol, benzylbenzoate, methylbenzoate, methylsalicylate, eugenol, isoeugenol, etc.) were reduced relative to control flowers (Figure 6B). The levels of some other volatiles were not affected by *EOBI* suppression (e.g., benzaldehyde, phenylethyl alcohol, and phenylethyl acetate). The level of the monoterpene limonene, as expected, was similar in RNAi-suppressed and control flowers.

To further detail the effect of *EOBI* silencing on scent production, we analyzed the expression levels of genes involved in floral scent production in EOBI-RNAi–suppressed flowers. Suppression of *EOBI* led to significant downregulation of transcripts from the shikimate pathway, as evidenced by significantly lower transcript levels of genes encoding 5-enol-pyruvylshikimate-3-phosphate synthase (*EPSPS*), 3-deoxy-D-arabinoheptulosonate-7-phosphate synthase (*DAHPS*), chorismate synthase (*CS*), chorismate mutase 1 (*CM1*), prephenate aminotransferase (*PPA-AT*), and arogenate dehydratase 1 (*ADT1*) in EOBI-RNAi–suppressed petunia flowers compared with control flowers (Figures 7A to 7F). Transcript levels of both *PAL1* and *PAL2*, representing core phenylpropanoid pathway genes, were also significantly downregulated in *EOBI*-silenced corollas compared with transgenic controls (Figures 7G and 7H). Levels of transcripts coding for enzymes that direct the production of specific phenylpropanoid scent volatiles (e.g., *S*-adenosyl-L-methionine:benzoic acid/salicylic acid carboxyl methyltransferase 1 and 2 [*BSMT1,2*], *IGS* and eugenol synthase [*EGS*]) were also downregulated in EOBI-RNAi versus control flowers (Figures 7J, 7K, 7M, and 7N); transcript levels of benzoyl CoA:benzyl alcohol/phenylethanol benzoyltransferase (*BPBT*) and coniferyl alcohol acyltransferase were not affected in *EOBI*-silenced flowers (Figures 7I and 7L).

Transcript levels of *ODO1* and *EOBII* in EOBI-RNAi versus control flowers were also analyzed to evaluate the interrelationships among regulatory factors affecting various branches leading to phenylpropanoid scent production (Figure 8). Silencing of *EOBI* did not affect *EOBII* transcript levels; on the other hand, transcript levels of *ODO1* were significantly downregulated in flowers of the EOBI-RNAi lines compared

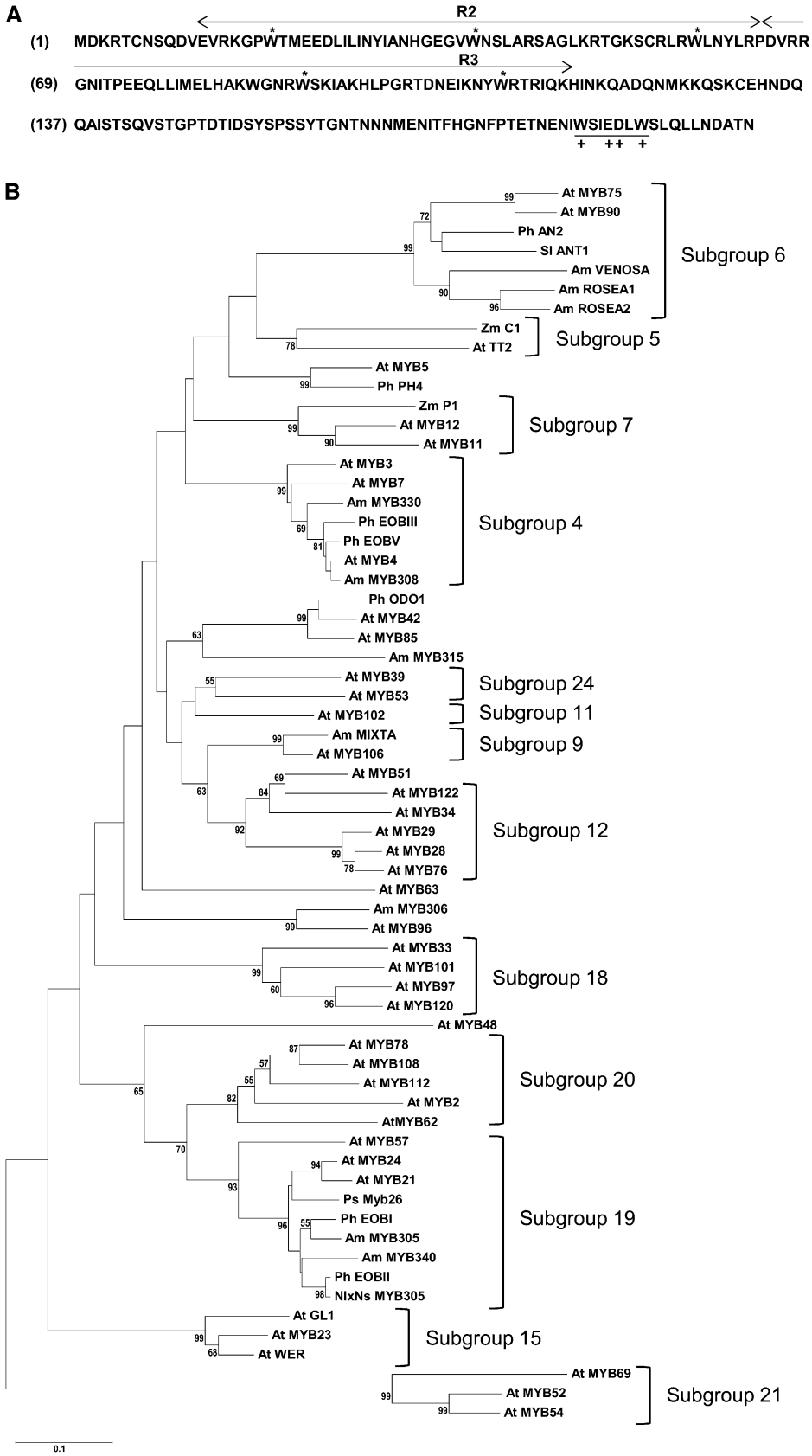

Figure 5. Structure and Phylogenetic Analyses of EOBI.

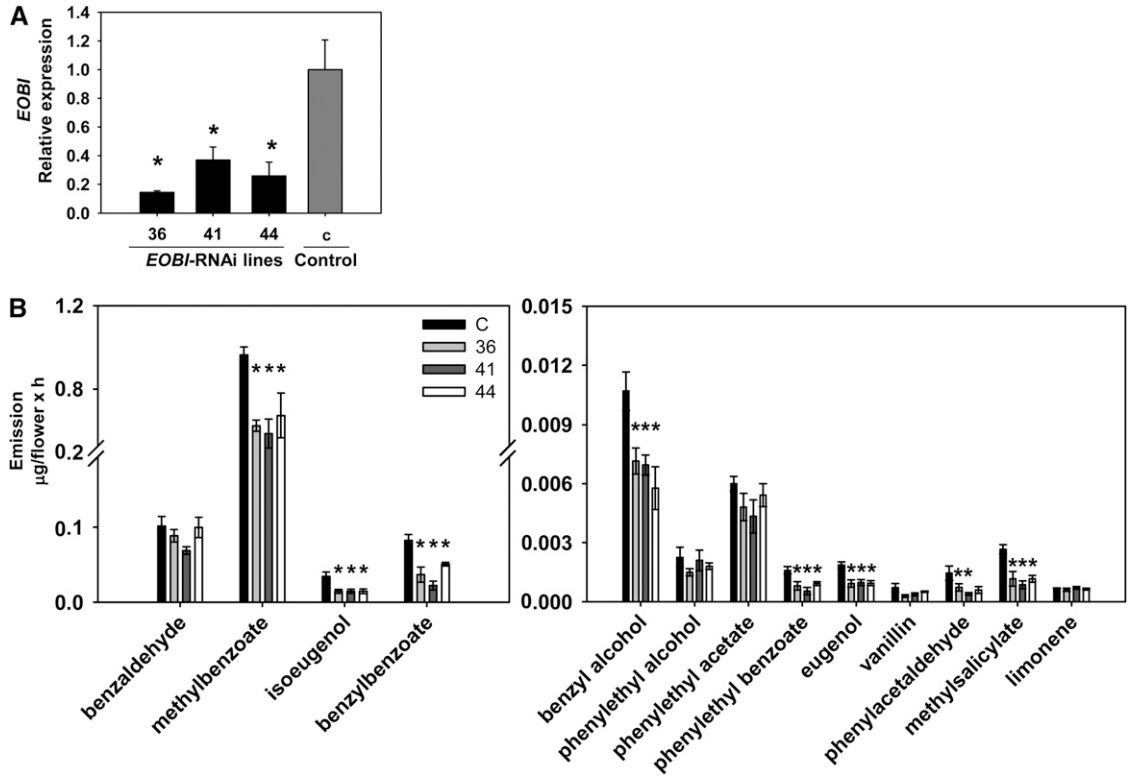

Figure 6. Suppression of *EOBI* Expression Reduces Levels of Volatile Phenylpropanoids in Petunia Flowers.

(A) Quantitative real-time PCR analysis of *EOBI* transcript levels in EOBI-RNAi corollas (transgenic lines 36, 41, and 44) compared with control $35S_{pro}$:GUS transgenic (c) corollas. Samples were collected from corollas at anthesis. Presented data (three biological replicates, each consisting of three technical repeats) were normalized to those from controls with SE indicated by vertical lines. Significance of differences ($P \leq 0.05$) between treatments and control (asterisks) was calculated based on the raw transcript level data normalized to *Actin* using Dunnett's method following ANOVA.

(B) Dynamic headspace analyses, followed by gas chromatography–mass spectrometry, were performed for 24 h (10:00 to 10:00) with flowers collected from EOBI-RNAi (lines 36, 41, and 44) and control $35S_{pro}$:GUS transgenic (c) petunia plants. Graphs represent the average of five independent replicates of major and minor volatiles (left and right graphs, respectively), with SE indicated by vertical lines. Significance of differences ($P \leq 0.05$) between treatments and control (asterisks) was calculated using Dunnett's method following ANOVA.

with control flowers (Figures 8A and 8B). Interestingly, analysis of petunia flowers with RNAi-suppressed *ODO1* (Figure 8C; Verdonk et al., 2005) revealed significantly upregulated *EOBI* transcript levels (Figure 8D), suggesting a negative feedback loop between EOBI and ODO1.

EOBI Activates Genes Involved in Phenylpropanoid Scent Production

To evaluate the ability of EOBI to transcriptionally activate scent-related genes, protoplasts cotransformed with $35S_{pro}$:EOBI and PAL_{pro}:DsRed or with $35S_{pro}$:EOBI and IGS_{pro}:DsRed constructs were employed (Figures 9Aa to 9Af). An unrelated MYB regulatory factor (MYBYS) under the control of the 35S promoter ($35S_{pro}$:MYBYS) or $35S_{pro}$:CFP were used as controls for promoter-activation analyses. Only protoplasts cotransformed with $35S_{pro}$:EOBI and IGS_{pro}:DsRed or with $35S_{pro}$:EOBI and PAL_{pro}:DsRed expressed DsRed (Figures 9Ab and 9Ae). Control protoplasts cotransformed with $35S_{pro}$:MYBYS or $35S_{pro}$:CFP instead of $35S_{pro}$:EOBI did not yield DsRed fluorescent signal when either PAL_{pro}:DsRed or IGS_{pro}:DsRed was used as the reporter (Figures 9Ah, 9Ak, 9An, and 9Aq). Overexpression

Figure 5. (continued).

(A) Protein sequence of petunia line P720 EOBI. The two MYB repeats (R2 and R3) are indicated by arrows, and the critical Trp residues are indicated by asterisks. The W/Y-MDDIW motif region is underlined (+ indicates conserved amino acids). Numbers in parentheses indicate amino acid positions.

(B) Phylogenetic tree displaying the similarity of EOBI to other R2R3-MYB proteins. Bootstrap values are indicated at branch nodes, and scale bar indicates the number of amino acid substitutions per site. Names of proteins are given in uppercase letters and their origin is indicated by a two-letter prefix: Am, *A. majus*; Ph, *P. hybrida*; NIxNs, *N. langsdorffii* × *N. sanderae*; Ps, *P. sativum*; At, *Arabidopsis*; Sl, *S. lycopersicum*; Zm, *Zea mays*. AN2, ANTHOCYANIN2; ANT1, ANTHOCYANIN1; C1, COLORLESS1; GL1, GLABRA1; TT2, TRANSPARENT TESTA2; WER, WEREWOLF. GenBank accession numbers are given in Supplemental Table 2 online. The alignment used to generate this tree is available as Supplemental Data Set 1 online.

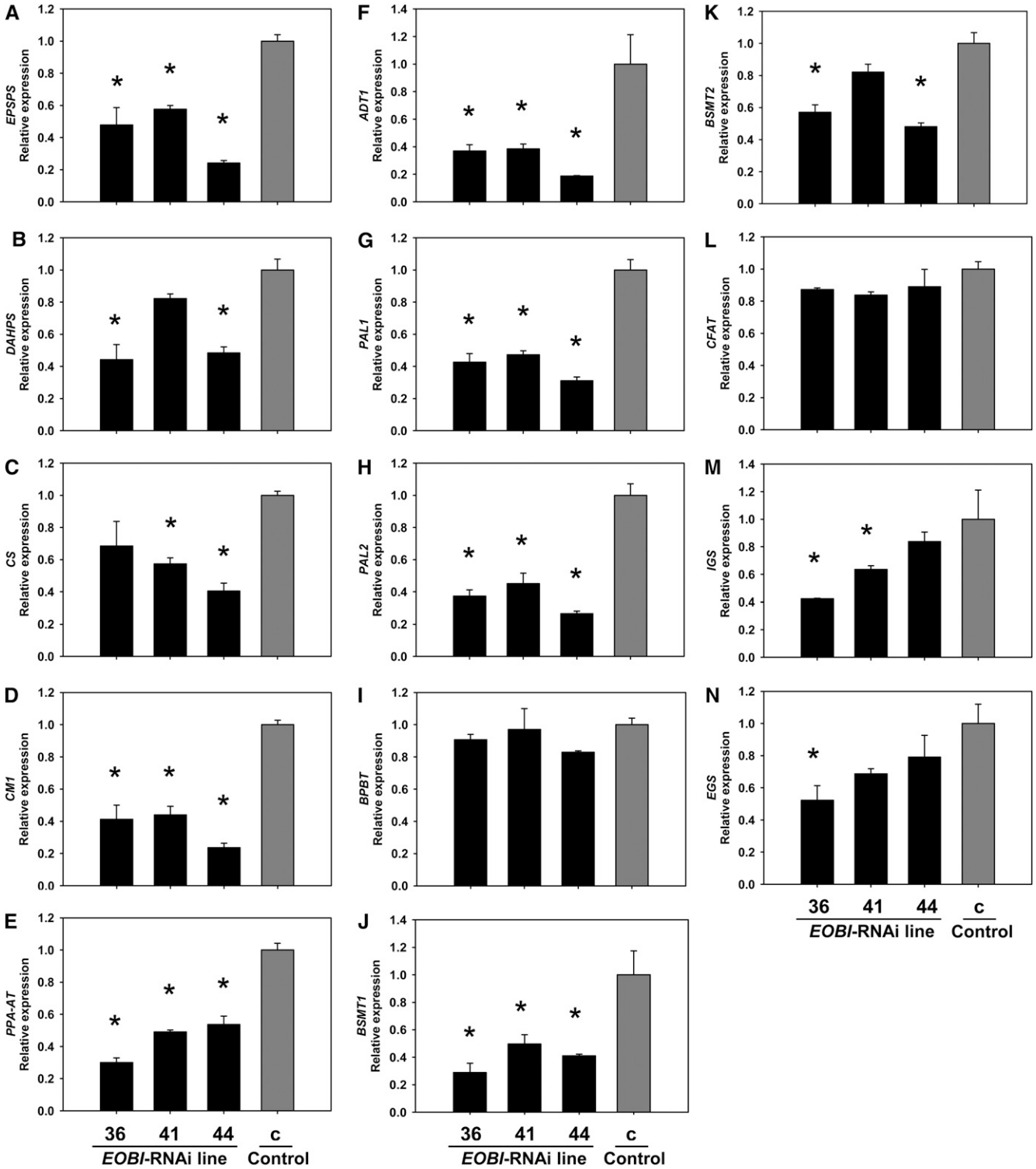

Figure 7. *EOBI* Silencing Leads to Downregulation of the Expression of Genes in the Shikimate and Phenylpropanoid Pathways.

Quantitative real-time PCR analysis of *EPSPS*, *DAHPS*, *CS*, *CM1*, *PPA-AT*, *ADT1*, *PAL1*, *PAL2*, *BPBT*, *BSMT1*, *BSMT2*, coniferyl alcohol acyltransferase, *IGS*, and *EGS* transcript levels, respectively, in EOBI-RNAi corollas (transgenic lines 36, 41, and 44) compared with control $35S_{pro}$:GUS transgenic (c) corollas. Samples were collected from corollas 1 d after anthesis. Presented data (three biological replicates, each consisting of three technical repeats) were normalized to those from control corollas with SE indicated by error bars. Significance of differences ($P \leq 0.05$) between treatments and control (asterisks) was calculated using Dunnett's method following ANOVA based on the raw transcript level data normalized to *Actin*.

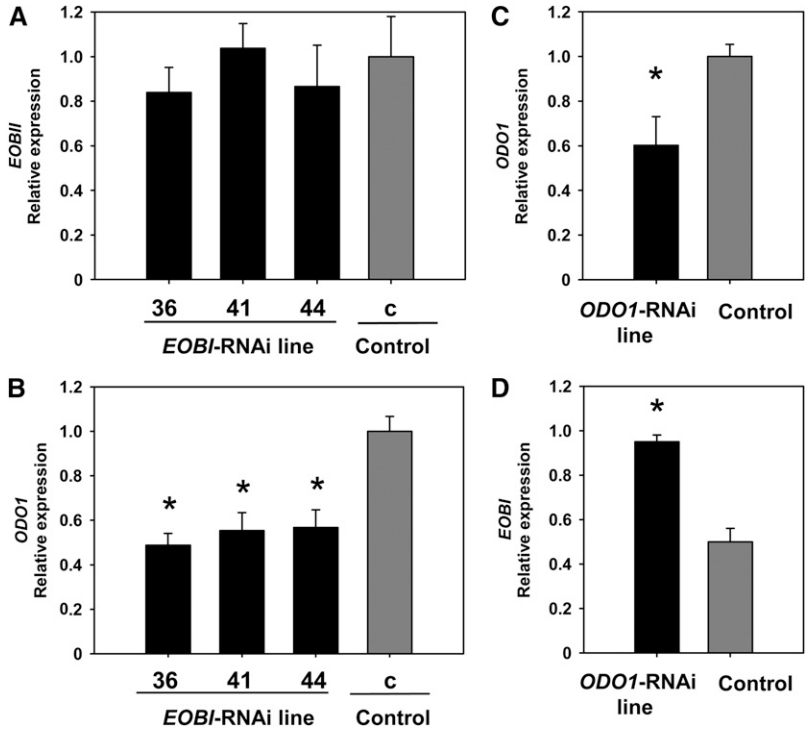

Figure 8. Interrelationship between EOBI and ODO1 Regulatory Factors.

(A) and **(B)** Quantitative real-time PCR analysis of *EOBII* and *ODO1* transcript levels, respectively, in EOBI-RNAi corollas at anthesis (transgenic lines 36, 41, and 44) compared with control $35S_{pro}$:GUS transgenic (c) corollas.

(C) and **(D)** Quantitative real-time PCR analysis of *ODO1* and *EOBI* transcript levels, respectively, in ODO1-RNAi petunia corollas compared with control $35S_{pro}$:GUS transgenic corollas. Samples were collected from corollas 1 d after anthesis. Presented data were normalized to those from control corollas with SE indicated by vertical lines. Significance of differences ($P \leq 0.05$; three to four biological replicates, each consisting of three technical repeats) between treatments and control (asterisks) was calculated using Dunnett's method following ANOVA based on the raw transcript level data normalized to *Actin*.

of EOBI in petunia leaves infiltrated with *Agrobacterium* carrying $35S_{pro}$:EOBI also led to activation of endogenous *IGS* in the inoculated tissues (see Supplemental Figure 4 online), further establishing the capacity of EOBI to activate *IGS* expression.

To evaluate the ability of EOBI to interact with *PAL* and *IGS* promoters, a yeast one-hybrid (Y1H) assay was performed using *EOBI* (pD22-EOBI) and *LacZ* driven by *PAL* or *IGS* promoter fragments (PAL_{pro}:GLacZi and IGS_{pro}:GLacZi, respectively) as targets. LacZ activity was detected in yeast harboring pD22-EOBI together with PAL_{pro}:GLacZi or IGS_{pro}:GLacZi, but not in control yeast harboring PAL_{pro}:GLacZi or IGS_{pro}:GLacZi together with pD22 lacking *EOBI* (Figure 9B).

Interaction of EOBI with the *ODO1* Promoter

To characterize the ability of EOBI to activate *ODO1*, petunia leaves were coinfiltrated with *Agrobacterium* harboring the $35S_{pro}$:EOBI construct together with a GUS reporter gene driven by the *ODO1* promoter ($ODO1_{pro}$:GUS; Van Moerkercke et al., 2011). Activation of $ODO1_{pro}$:GUS by EOBI was revealed in these co-inoculated leaves; no GUS activity was detected in control tissues coinoculated with $35S_{pro}$:YFP (instead of EOBI) and $ODO1_{pro}$:GUS (Figure 10A). To further assay the interaction between EOBI and the *ODO1* promoter, two complementary approaches, Y1H and EMSA, were employed. The Y1H assay was performed using pD22-EOBI and *LacZ* driven by the *ODO1* promoter fragment ($ODO1_{fpro}$:GLacZi) containing two MYB binding sites (Van Moerkercke et al., 2011). LacZ activity was detected in yeast harboring pD22-EOBI together with $ODO1_{fpro}$:GLacZi and not in control yeast harboring $ODO1_{fpro}$:GLacZi together with pD22 lacking *EOBI* (Figure 10B). To analyze protein-DNA complex formation using EMSA, EOBI recombinant protein (fused to MBP) was incubated with labeled $ODO1_{fpro}$, with or without competitor DNA. Gel-shift assays (Figure 10C) showed that EOBI recombinant protein can interact with the *ODO1* promoter. Unlabeled $ODO1_{fpro}$ was able to compete with the labeled $ODO1_{fpro}$ for EOBI binding in a dose-dependent manner, and the mobility shift was not seen in control reactions lacking EOBI, indicating a specific interaction between EOBI and the *ODO1* promoter.

DISCUSSION

The importance of floral scent in the plant's life cycle on the one hand, and the high energy cost invested in metabolism of these volatiles on the other, probably explain the need for tight control

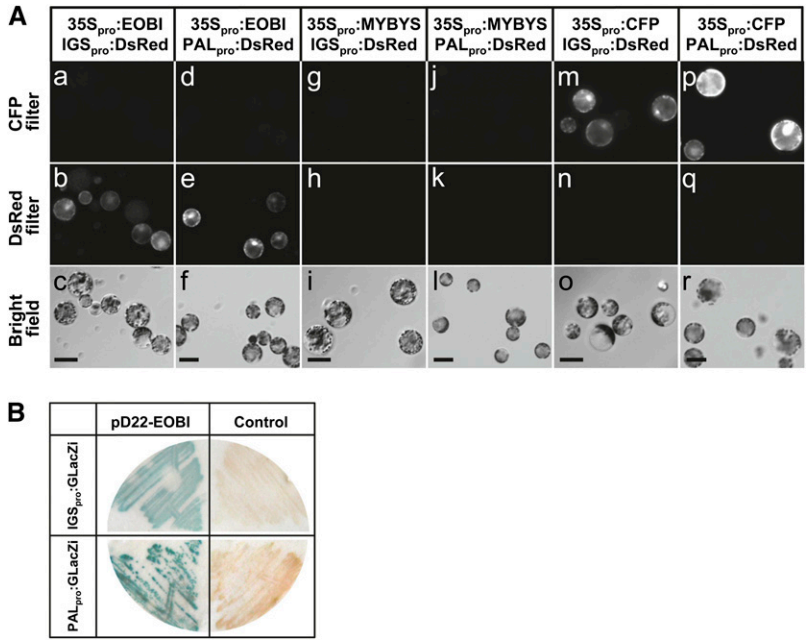

Figure 9. EOBI Interacts with and Activates *IGS* and *PAL* Promoters.

(A) *Arabidopsis* protoplasts transformed with 35S-driven *EOBI* (35S$_{pro}$:EOBI) together with DsRed driven by the petunia *IGS* promoter (IGS$_{pro}$:DsRed) (**[a]** to **[c]**) or with 35S$_{pro}$:EOBI together with DsRed driven by the *PAL* promoter (PAL$_{pro}$:DsRed) (**[d]** to **[f]**). As controls, protoplasts were transformed with IGS$_{pro}$:DsRed or PAL$_{pro}$:DsRed together with cucumber *MYBYS* driven by the 35S promoter (35S$_{pro}$:MYBYS) (**[g]** to **[i]** and **[j]** to **[l]**, respectively) or with 35S$_{pro}$:CFP (**[m]** to **[o]** and **[p]** to **[r]**, respectively). CFP, DsRed, and bright-field images are shown in top, middle and bottom panels, respectively. Bars = 50 μm.

(B) Interaction of EOBI with *IGS* and *PAL* promoters as revealed by Y1H analysis. The interaction of EOBI protein, fused to GAL4 activation domain (pD22-EOBI), with *LacZ* driven by *IGS* (IGS$_{pro}$:GLacZi) or *PAL* (PAL$_{pro}$:GLacZi) promoter is shown in the top and bottom left panels, respectively. Yeast transformed with IGS$_{pro}$:GLacZi or PAL$_{pro}$:GLacZi together with empty, *EOBI*-lacking pD22 (top and bottom right panels, respectively) were used as controls.

[See online article for color version of this figure.]

of this trait. To allow plasticity of the multistep metabolic pathways leading to floral scent, simultaneous regulation of elements at different junctions is likely to be required. The effect of EOBI on floral scent was demonstrated in both stably and transiently transformed plants. For example, *EOBI* silencing via transgenesis led to downregulation of numerous genes from the shikimate pathway and downstream scent-related genes from the phenylpropanoid pathway (i.e., *EPSPS*, *DAHPS*, *CS*, *CM1*, *ADT1*, and *PPA-AT*, and *PAL*, *IGS*, and *BSMT*, respectively). In some of the lines, the effect of *EOBI* silencing on a number of the target genes, such as *DAHPS*, *CS*, and *BSMT2*, was not significant, probably due to specific environment–genotype interactions or intragenotype variation of the highly complex trait that is scent. Indeed, variation in the expression levels of scent-related genes within populations of transgenic lines has been documented in *ADT1*- and *ODO1*-silenced petunia flowers; a similar lack of uniformity among individual plants was also apparent in studies of volatiles emitted by *cinnamate*:*CoA ligase*– and *3-ketoacyl-CoA thiolase*–silenced petunia lines (Verdonk et al., 2005; Van Moerkercke et al., 2009; Maeda et al., 2010; Klempien et al., 2012). *EOBI* silencing led to reduced levels of numerous floral volatiles (e.g., methylbenzoate, isoeugenol, benzylbenzoate, benzyl alcohol, phenylethylbenzoate, and others). In the case of benzylbenzoate, a reduction in emission levels despite a lack of effect on *BPBT* transcript levels might be ascribed to insufficient flow of substrates to this metabolic branch. A similar trend has been seen in flowers with suppressed *ODO1* (i.e., whereas *BSMT* transcript was not downregulated, the level of emitted methylbenzoate was reduced) (Verdonk et al., 2005). By contrast, while reduced in *EOBII*-suppressed flowers (Spitzer-Rimon et al., 2010), benzaldehyde levels were not affected in *EOBI*-silenced flowers. Since the biosynthetic steps leading to benzaldehyde production have not yet been deciphered (Klempien et al., 2012), we cannot exclude the possibility that the relevant enzymes are affected by suppression of *EOBII* but not *EOBI*; alternatively, metabolic flow toward benzaldehyde may be in excess relative to the downstream steps; in transgenic flowers in which these downstream steps are strongly downregulated, benzaldehyde levels would be less affected (Boatright et al., 2004).

Complex interactions between transcription factors, including MYBs, have been demonstrated in numerous plant systems for an array of processes (Jin and Martin, 1999; Aharoni et al., 2001; Koes et al., 2005; Schwinn et al., 2006; Kaufmann et al., 2010; Sønderby et al., 2010). Several lines of evidence presented here support EOBII's involvement in transcriptional activation of *EOBI* expression as well. These include the negative and positive

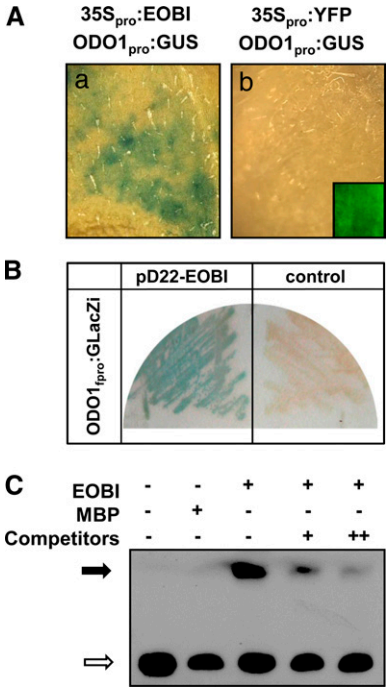

Figure 10. EOBI Binds to and Activates the *ODO1* Promoter.

(A) *ODO1* promoter activity in petunia leaves 48 h after coinfiltration with agrobacteria carrying *GUS* driven by the *ODO1* promoter (ODO1$_{pro}$:GUS; Van Moerkercke et al., 2011) together with 35S promoter–driven *EOBI* (35S$_{pro}$:EOBI) **(a)** or *YFP* driven by the 35S promoter (35S$_{pro}$:YFP) as a control **(b)**. Inset in **(b)** shows YFP control image.

(B) Interaction of EOBI with *ODO1* promoter as revealed by Y1H analysis. Interaction of EOBI protein, fused to GAL4 activation domain (pD22-EOBI), with *LacZ* driven by the *ODO1* promoter fragment (ODO1$_{fpro}$:GLacZi) is shown in left panel. Yeast transformed with ODO1$_{fpro}$:GLacZi together with empty EOBI-lacking pD22 (right panel) were used as a control.

(C) EMSA of an *ODO1* promoter fragment by EOBI. A biotinylated *ODO1* promoter fragment was used as the probe. MBP was used as a control protein. Black arrow indicates protein-DNA complexes. White arrow shows the positions of the free probe (bottom left). In lanes with competitor DNA, + and ++ indicate 200× and 1000× molar excess of non-labeled probe, respectively.

[See online article for color version of this figure.]

effects of *EOBII* silencing and overexpression on *EOBI* transcript levels, respectively, and EOBII's ability to bind the *EOBI* promoter in vitro and to activate it in leaf protoplasts. The spatial, developmental, and temporal accumulation patterns of *EOBI* transcript relative to *EOBII* further support the relationship between these factors (Figures 3 and 11; Spitzer-Rimon et al., 2010). Expression of both genes was flower specific, with maximum transcript levels in the limbs. This tissue specificity is probably transcriptionally regulated, since a similar expression pattern was revealed when a reporter gene driven by the *EOBI* promoter was expressed in different petunia tissues (Figure 4A). With respect to developmental expression pattern, *EOBII* transcript accumulation precedes that of *EOBI*, yet expression of both genes peaks at anthesis (Figure 3B; Spitzer-Rimon et al., 2010). Similarly, analyses of diurnal accumulation of *EOBI* transcript showed that it follows that of *EOBII*: *EOBII* transcript starts to accumulate from 15:00 onward, whereas accumulation of *EOBI* transcript becomes apparent after midnight. As might be expected for a scent regulator, the expression pattern of *EOBI* is rhythmic, with a phase preceding that of biosynthetic floral scent-related genes and that of scent production: Maximal levels of the transcript were detected from the early morning hours until noon, preceding, for example, peak *CM*, *DAHPS*, *PPA-AT*, and *IGS* transcript accumulation (Colquhoun et al., 2010; Maeda et al., 2011) by 5 to 6 h. A similar lag was observed in *EOBI* versus *ODO1* expression, with activity of the *ODO1* promoter being highest at 15:00 (Van Moerkercke et al., 2011). Transcriptional activation by EOBI of *ODO1* and the structural biosynthetic genes *IGS* and *PAL* is in agreement with the hierarchical and sequential activation of the pathway toward scent production in flowers.

EOBI's effect on *ODO1* expression, its interaction with *ODO1* promoter, and its developmental pattern of expression support its role as a key factor, in addition to EOBII, for correct expression of *ODO1*. Interestingly, while EOBI activates *ODO1* expression, the latter negatively affects *EOBI* levels as revealed by analyses of *EOBI* transcript levels in flowers of ODO1-RNAi transgenic petunia. This could explain the increased transcript levels of *BSMT* in ODO1-RNAi lines (Verdonk et al., 2005), since the *BSMT* transcript level is positively affected by *EOBI*. The negative feedback loop between ODO1 and EOBI may represent fine-level control in the scent regulation web. For example, such a feedback loop might allow continual correction of ODO1 levels according to EOBI levels and vice versa, leading to the coordination of flux into the pathway with that of the final enzymatic steps of the scent molecule's production; in this way, tight control of resources expended by plants for activation of primary and specialized branches (i.e., production of volatile phenylpropanoids) can be achieved. A similar regulatory genetic loop was recently described in the pathway leading to aliphatic glucosinolate production (Sønderby et al., 2010).

Complex transcriptional control of metabolic networks has been described in several plant systems. For example, in petunia, flavonoid biosynthesis and vacuolar acidification are regulated by a complex network of interactions between MYB–basic helix-loop-helix (bHLH)–WD40 proteins. While binding of bHLH–ANTOCYANIN1 to PH4 activates vacuolar acidification, its interaction with AN2 regulates anthocyanin synthesis (Spelt et al., 2000; Koes et al., 2005; Quattrocchio et al., 2006). The transcriptional regulation network of ripening-related metabolism has been demonstrated in tomato (*Solanum lycopersicum*) fruits through interactions of NON-RIPENING, RIPENING-INHIBITOR, and COLORLESS NON-RIPENING factors with APETALA2a, which not only governs chromoplast differentiation and ethylene production, but also regulates cell wall biosynthesis, amino acid production, and secondary metabolism (Karlova et al., 2011). EOBI was also found to regulate the transcription of genes involved in both primary and secondary metabolism (i.e., aromatic amino acid synthesis and scent production). Interestingly, EOBII, which directly regulates both *EOBI* and *ODO1*, has been suggested to play a more complex role in flower development, particularly during the stages preceding flower opening (Colquhoun

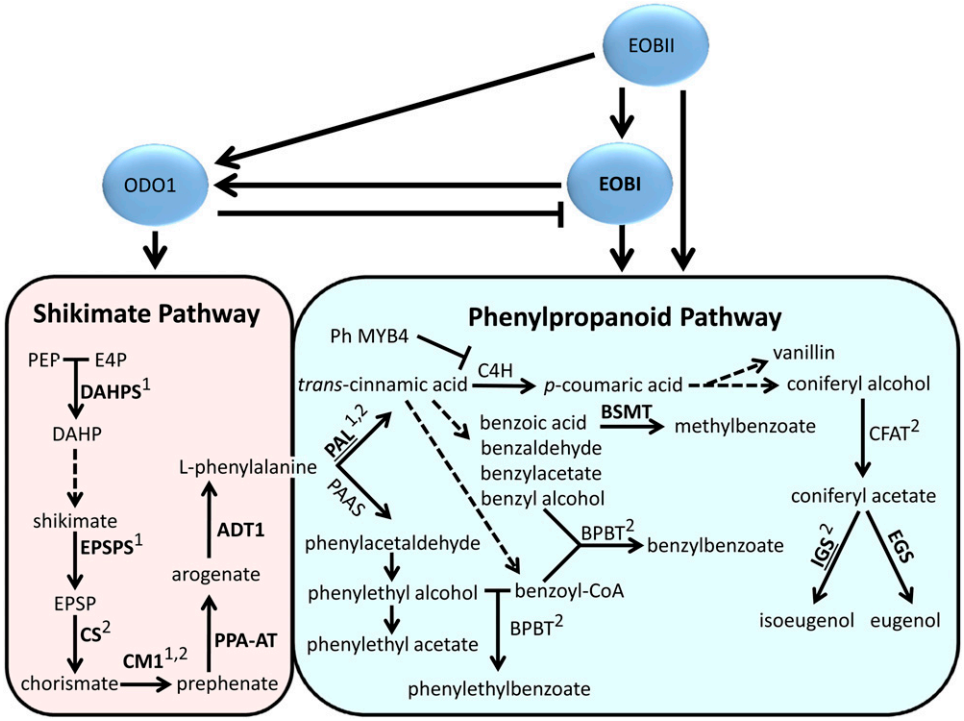

Figure 11. Regulation of Scent in Petunia Flowers: Schematic Diagram.

Solid arrows represent a one-step enzymatic reaction, and dashed arrows represent several enzymatic reactions or as yet undescribed steps. Genes downregulated following suppression of *EOBI*, *ODO1*, or *EOBII* are in boldface or marked by a superscript one or two, respectively. *IGS* and *PAL*, shown to interact with EOBI and EOBII, are underlined. BPBT, benzoyl-CoA:benzyl alcohol/2-phenylethanol benzoyltransferase; BSMT, *S*-adenosyl-L-Met: benzoic acid/salicylic acid carboxyl methyltransferase; C4H, cinnamate-4-hydroxylase; CFAT, coniferyl alcohol acetyltransferase; CS, chorismate synthase; DAHP, 3-deoxy-D-arabino-heptulosonic acid 7-phosphate; E4P, D-erythrose-4-phosphate; EGS, eugenol synthase; EPSP, 5-enolpyruvate-shikimate-3-phosphate; IGS, isoeugenol synthase; PAAS, phenylacetaldehyde synthase; PEP, phosphoenolpyruvate.
[See online article for color version of this figure.]

et al., 2011b). These interrelationships reinforce the tight link between primary metabolism, secondary metabolism, and flower development.

The interplay between machineries controlling primary and specialized metabolic branches is not surprising, especially based on the progressive evolution of pathways (for example, recruitment of enzymes from primary metabolism to the phenylpropanoid pathway) in land plants (Stafford, 1991; Ferrer et al., 2008). The R2R3-MYB family of transcription factors that, in complex with other factors (e.g., bHLH and WD40 factors), regulates most of the enzymatic steps in the phenylpropanoid pathway, underwent dramatic expansion around the time of land colonization by plants (Dubos et al., 2010; Feller et al., 2011). According to *Arabidopsis* classification, R2R3-MYB transcription factors are commonly divided, based on C-terminal domains, into ~22 subgroups (Kranz et al., 1998; Dubos et al., 2010). The variations in the numbers and sizes of the subgroups between species attests to gene specialization after divergence from the last common ancestor (Zhang et al., 2000; Dias et al., 2003; Wilkins et al., 2009; Feller et al., 2011). The growth and specialization of the R2R3-MYB family members can be exemplified by many processes involved in the adaptation of land plants, for example, secondary wall biosynthesis, UV protection, showy flower traits, pollinator attraction, etc. (Dubos et al., 2010; Feller et al., 2011). EOBI falls into subgroup 19, together with MYB305 from snapdragon and ornamental tobacco, EOBII from petunia, and other phenylpropanoid-associated MYB factors (Sablowski et al., 1994; Moyano et al., 1996; Uimari and Strommer, 1997; Shin et al., 2002; Li et al., 2006). EOBI shows higher sequence similarity to MYB305 from snapdragon than to petunia EOBII (Figure 5; see Supplemental Figure 5 online); the latter shares highest sequence similarity with MYB305 from ornamental tobacco, suggesting that EOBI and EOBII diverged relatively early in evolution. Interestingly, although snapdragon flowers emit phenylpropanoid volatiles during the day, whereas petunia flowers emit them during the night, similar molecular mechanisms have been suggested for the control of methylbenzoate emission in these plant systems (Kolosova et al., 2001); it is tempting to speculate that the interplay between the EOBI and II homologs in *Antirrhinum*, MYB305 and MYB340, respectively, is involved in the regulation of scent production in snapdragon, possibly via regulation of PAL expression.

Promoters of at least two genes encoding phenylpropanoid scent-related enzymes, *IGS* and *PAL*, interact with and are transactivated by both EOBI and EOBII. Partial redundancy within subgroup 19 MYB factors has been previously demonstrated. In

snapdragon, for example, both MYB305 and MYB340 can activate the promoter region of phenylpropanoid genes *PAL2*, chalcone isomerase (*CHI*), and flavonone 3-hydroxylase (Moyano et al., 1996). Transcriptional activation of the target *CHI* promoter by MYB340 is stronger than that of MYB305, but the DNA binding activity of MYB305 is stronger than that of MYB340. These multiple interactions have been suggested to enable fine-tuning of the target genes' transcriptional activation (Moyano et al., 1996).

Transactivation of one R2R3-MYB by another one belonging to the same or a different subgroup may represent an additional general feature of R2R3-MYB factors that enables further amplification and diversification of the outcome signal (Kang et al., 2009; Sønderby et al., 2010, Zhong et al., 2010). Such a feed-forward mechanism has been shown for members of subgroups 15 and 12: Members of the latter group, MYB28 and MYB76, positively regulate MYB29, while WERWOLF feeds forward on MYB23 (Kang et al., 2009; Sønderby et al., 2010). Similarly, EOBII transcriptionally activates *EOBI*, and both EOBI and EOBII activate the expression of the distantly related *ODO1*, which in turn negatively affects *EOBI* transcription (Figure 11). Hence, the genetic relationships between EOBI, EOBII, and ODO1 may also serve as a dynamic regulatory tool to adjust metabolic flow. This is likely to be particularly important when dealing with processes that carry a high metabolic cost.

METHODS

Plant Material

Rooted petunia plantlets (*Petunia hybrida* lines P720 and W115 [cv Mitchell]) were obtained from Danziger-"Dan" Flower Farm (Mishmar Hashiva, Israel). Transgenic cv Mitchell (W115) with RNAi-suppressed *ODO1* (Verdonk et al., 2005) was kindly provided by Robert C. Schuurink, University of Amsterdam, The Netherlands. All plants were grown in the greenhouse under 25°C/20°C day/night temperatures and natural photoperiod.

Cloning of *EOBI* and Construction of Vectors

MYB-like DNA fragments termed *R2R3-EOBI*, *R2R3-EOBIII*, and *R2R3-EOBV* were isolated by RT-PCR as described previously (Spitzer-Rimon et al., 2010). To clone the 3′ region of *EOBI*, a SMART RACE cDNA amplification kit (Clontech) was used. PCR was performed on petunia flowers' cDNA using a forward primer based on the sequence of *R2R3-EOBI* (see Supplemental Table 1 online, forward primer of set 1) and the kit's reverse primer. To clone the 5′ region of *EOBI*, PCR was performed on a petunia cDNA library using primers based on the sequence of the 3′-*EOBI* (see Supplemental Table 1 online, reverse primer of set 1). The full-length *EOBI* was cloned from petunia lines P720 and W115 using primers to the 5′ and 3′ ends of the partial *EOBI* sequences (see Supplemental Figure 6 online). To generate *Tobacco rattle virus* (TRV2) containing the 3′ untranslated region of *EOBI* (TRV2-EOBI), 85 bp of line P720 *EOBI* were PCR amplified using primer set 2. To generate pTRV2 containing the 5′ region of *EOBIII* (TRV2-EOBIII), 79 bp of line P720 *EOBIII* were PCR amplified using primer set 3. To generate pTRV2 containing the 3′ region of *EOBV* (TRV2-EOBV), 206 bp of line P720 *EOBV* were PCR amplified using primer set 4. To construct pTRV2 with *EOBI* fused upstream of GFP (pTRV2-EOBI:GFP), the 606-bp ORF of line P720 *EOBI* was PCR amplified using primer set 5 (containing additional Gly-Gly amino acids at the 5′ end of the reverse primer), and ligated (in-frame with GFP) into pTRV2-GFP (Spitzer et al., 2007), which was restricted with *Hpa*I at the 3′ end of *GFP*. The pTRV2 derivatives described above and pTRV1 were then transfected into *Agrobacterium tumefaciens* (strain AGLO) and used for plant inoculation as described by Spitzer et al. (2007). To generate a binary vector containing *EOBI* under the control of the cauliflower mosaic virus 35S promoter ($35S_{pro}$:EOBI), the full-length *EOBI* of line P720 was PCR amplified using primer set 6. The PCR product was cloned into a pCd shuttle vector between the cauliflower mosaic virus 35S promoter and octopine synthase terminator; the resultant plasmid was then digested with *Kpn*I-*Xba*I and the generated restriction fragment was inserted into binary vector pCGN1559 containing the *neomycin phosphotransferase II* gene (Ben Zvi et al., 2008). To generate transgenic EOBI- and EOBII-RNAi petunia plants, 157- and 197-bp fragments from the 3′ ends of *EOBI* and *EOBII*, respectively, were obtained by PCR, using primer set 7 for *EOBI* and primer set 8 for *EOBII*. The PCR fragments were cloned into pRNA69 in sense and antisense orientations, separated by an intron, as described by Leitner-Dagan et al. (2006). The constructs were then cloned into the *Not*I site of the binary vector pART27 and transformed into *Agrobacterium* strain AGLO.

Plant Transformation and Regeneration

Petunia variety W115 (cv Mitchell) was used to generate transgenic plants by modified leaf-disk transformation as described by Guterman et al. (2006). Petioles were incubated in bacterial suspension for 10 min and then transferred to cocultivation medium (4.4 g/L Murashige and Skoog [MS] basal medium [Sigma-Aldrich] supplemented with 30 g/L Suc and 7 g/L oxoid agar [Sigma-Aldrich], 0.5 mg/L benzyladenine, and 0.01 mg/L 1-naphthalene acetic acid [NAA]) for 2 d in the dark. Regeneration and selection of shoots were conducted on MS with 1.5 mg/L benzyladenine, 0.1 mg/L NAA, 0.1 g/L gibberellin, 300 mg/L carbenicillin, and 80 mg/L kanamycin. Fully developed shoots were transferred to elongation medium (MS with 0.5 mg/L zeatin, 100 mg/L carbenicillin, 200 mg/L cefataxime, and 80 mg/L kanamycin). Plants were rooted on MS with 0.1 mg/L NAA, 100 mg/L carbenicillin, 200 mg/L cefataxime, and 50 mg/L kanamycin.

Agroinoculation of TRV Vectors

Agrobacterium (strain AGLO) transformed with pTRV1 and pTRV2 derivatives was prepared as described previously (Liu et al., 2002). The *Agrobacterium* culture was grown overnight at 28°C in Luria-Bertani medium with 50 mg/L kanamycin and 200 μM acetosyringone. The cells were harvested and resuspended in inoculation buffer containing 10 mM MES, pH 5.5, 200 μM acetosyringone, and 10 mM $MgCl_2$ to an OD_{550} of 10. Following an additional 3 h of incubation at 28°C, the bacteria containing pTRV1 were mixed with those containing the pTRV2 derivatives in a 1:1 ratio; 200 to 400 μL of this mixture was applied to the cut surface, after removing the apical meristem, of petunia line P720 plantlets. For subcellular localization of EOBI, 3-week-old seedlings of *N. benthamiana* were agroinfected with pTRV2-EOBI:GFP and pTRV2-GFP by leaf infiltration using a syringe (Spitzer-Rimon et al., 2010). Transient expression of GFP in the tobacco (*Nicotiana benthamiana*) epidermis was evaluated 36 h after infection using an epifluorescence inverted microscope (Olympus-IX8 Cell-R) with a 12-bit Orca-AG charge-coupled device camera (Hamamatsu).

Protoplast Transformation

To clone the *EOBI* and *EOBII* promoter regions from petunia line W115, the Genome-Walker kit (Clontech) was used according to the manufacturer's instructions and as described by Spitzer-Rimon et al. (2010). EOBI (1302 bp) and EOBII (1343 bp) promoter regions were cloned upstream of DsRed ($EOBI_{pro}$:DsRed and $EOBII_{pro}$:DsRed) into *Kpn*I and *Bam*HI sites (forward primer 5′-GGTACCGTATGTTGAAAGGGCAGCCT-3′ and reverse primer 5′-GGATCCGATATAGGATTTTGACGAGGAACT-AAT-3′) of pSAT6A-DsRed2-N1 vector (Spitzer-Rimon et al., 2010). Protoplasts were isolated from *Arabidopsis thaliana* and petunia line P720 leaf mesophyll and employed for transient expression, using the polyethylene glycol transformation method (Locatelli et al., 2003), of

$35S_{pro}$:EOBI and IGS_{pro}:DsRed (Spitzer-Rimon et al., 2010), $35S_{pro}$:EOBI and PAL_{pro}:DsRed (Spitzer-Rimon et al., 2010), $35S_{pro}$:EOBII and $EOBI_{pro}$:DsRed, or $35S_{pro}$:EOBI and $EOBII_{pro}$:DsRed. Protoplasts transformed with IGS_{pro}:DsRed and pSAT6-ECFP-C1 ($35S_{pro}$:CFP; Tzfira et al., 2005), IGS_{pro}:DsRed and $35S_{pro}$:MYBYS (Leitner-Dagan et al., 2006), PAL_{pro}:DsRed and $35S_{pro}$:CFP, PAL_{pro}:DsRed and $35S_{pro}$:MYBYS, $EOBI_{pro}$:DsRed and $35S_{pro}$:CFP, or $EOBI_{pro}$:DsRed and $35S_{pro}$:MYBYS were used as controls. Imaging was performed by epifluorescence inverted microscope 14 h after transformation, with the charge-coupled device camera.

Transient Overexpression in Petunia

Transient overexpression in petunia line W115 leaves and flowers was performed according to Long et al. (2009). Petunia buds 3 d before anthesis were vacuum infiltrated with *Agrobacterium* containing $35S_{pro}$:EOBII or $35S_{pro}$:GUS. RNA was extracted from infiltrated corollas 48 h after inoculation, and the transcript levels of selected genes were analyzed by real-time RT-PCR. For promoter analyses, $EOBI_{pro}$:DsRed and IGS_{pro}:DsRed were cloned into the pCGN1559 binary vector to create pCGN1559-$EOBI_{pro}$:DsRed and pCGN1559-IGS_{pro}:DsRed, respectively. Flowers (3-cm buds and flowers at anthesis) and leaves were coinfiltrated, as described above, with *Agrobacterium* AGLO carrying pCGN1559-$EOBI_{pro}$:DsRed or pCGN1559-IGS_{pro}:DsRed together with strain AGLO carrying pART27-$35S_{pro}$:YFP (kindly provided by Yuval Eshed, Weizmann Institute, Rehovot, Israel). After 36 h, the leaves and flowers were examined using a fluorescence binocular microscope (FLOUIII; Leica) under white and UV light with DsRed and YFP filters. *Agrobacterium* AGLO carrying pCGN1559-IGS_{pro}:DsRed or pBIN-$M19_{pro}$:GUS ($ODO1_{pro}$:GUS; Van Moerkercke et al., 2011) and pCGN1559-$35S_{pro}$:EOBI was used for expression of *EOBI* in petunia leaves. pCGN1559-$35S_{pro}$:EOBI was substituted with pART27-$35S_{pro}$:YFP in control experiments. After 2 to 5 d, the leaves were examined with a fluorescence binocular microscope and by quantitative real-time PCR.

GUS activity was assayed by incubating tissue samples overnight at 37°C in a 0.1% (w/v) X-Gluc (5-bromo-4-chloro-3-indolyl β-D-glucuronic acid sodium salt; Biosynth) solution containing 0.1 M sodium phosphate buffer, pH 7.0, 10 mM EDTA, and 0.1% (w/v) Triton X-100. Green tissues were bleached, after staining, by immersion in 50% ethanol for a few hours, followed by several washes with 70% ethanol.

Real-Time PCR Analysis

Petunia total RNA was extracted with the Tri-Reagent kit (Molecular Research Center) and treated with RNase-free DNase (Fermentas). First-strand cDNA was synthesized using 1 μg total RNA, oligo(dT) primer, and Reverse Transcriptase ImProm-II (Promega). Real-time quantitative PCR was performed as described by Spitzer-Rimon et al. (2010) for 40 cycles (94°C for 15 min and then cycling at 94°C for 10 s, 60°C for 30 s, and 72°C for 20 s) in the presence of Absolute Blue qPCR SYBR Green ROX Mix (Thermo Fisher Scientific) on a Corbett Research Rotor-Gene 6000 cycler. A standard curve was generated for each gene using dilutions of cDNA samples, and data analysis were performed using Rotor-Gene 6000 series software 1.7. PCR primers used for amplification of gene-specific regions (at least one of the primers was directed to the UTR of the transcript) are listed in Supplemental Table 1 online, primer sets 9 to 28. Primer specificity was determined by melting curve analysis; a single, sharp peak in the melting curve ensured that a single, specific DNA species had been amplified.

Collection and Gas Chromatography–Mass Spectrometry Analysis of Volatile Compounds

For dynamic headspace analysis, flowers were collected 1 d after anthesis at 10:00, unless otherwise indicated. Volatiles emitted from detached petunia flowers were collected for 24 h using an adsorbent trap consisting of a glass tube containing 100 mg Porapak Type Q polymer (80/100 mesh; Alltech) and 100 mg charcoal-activated 20/40 mesh (Supelco), held in place with plugs of silanized glass wool (Guterman et al., 2006). Trapped volatiles were eluted using 1.5 mL hexane, and 2 μg iso-butylbenzene was added to each sample as an internal standard.

Gas chromatography–mass spectrometry analysis (1-μL sample) was performed using a device composed of a Pal autosampler (CTC Analytic), a TRACE GC 2000 equipped with an Rtx-5SIL mass spectrometer (Restek; i.d. 0.25 μm, 30 m × 0.25 mm) fused-silica capillary column, and a TRACE DSQ quadrupole mass spectrometer (ThermoFinnigan). Helium was used as the carrier gas at a flow rate of 0.9 mL/min. The injection temperature was set to 250°C (splitless mode) and the interface to 240°C, and the ion source was adjusted to 200°C. The analysis was performed under the following temperature program: 2 min of isothermal heating at 40°C followed by a 10°C/min oven temperature ramp to 250°C. The system was equilibrated for 1 min at 70°C before injection of the next sample. Mass spectra were recorded at 3.15 scan/s with a scanning range of 40 to 450 mass-to-charge ratio and electron energy of 70 eV. Compounds were tentatively identified (>95% match) based on the NIST/EPA/NIH Mass Spectral Library (data version NIST 05; software version 2.0d) using the XCALIBUR v1.3 program (ThermoFinnigan). Further identification of major compounds was based on comparison of mass spectra and retention times with those of authentic standards (Sigma-Aldrich) analyzed under similar conditions.

EMSA

MBP-EOBI and MBP-EOBII fusion proteins (cloned from $35S_{pro}$:EOBI and $35S_{pro}$:EOBII, respectively) were expressed in *Escherichia coli* cells essentially as done by Van Moerkercke et al. (2011). Four hours after induction with 0.1 mM isopropyl β-D-thiogalactopyranoside, the culture was harvested by centrifugation for 5 min at 5000*g*. The pellet was resuspended in 50 mL ice-cold MBP buffer (10 mM Tris-Cl, pH 7.5, 30 mM NaCl, 1 mM EDTA, 1 mM PMSF, and 1× protease inhibitor cocktail), sonicated for 15 min, and centrifuged for 20 min at 14,000*g*. The supernatant was incubated for 2 h at 4°C with prewashed amylose resin (NEB). The resin was then washed five times with 10 mM Tris-Cl, pH 7.5, and 1 M NaCl buffer. MBP, MBP-EOBI, and MBP-EOBII proteins were eluted with 10 mM Tris-Cl, pH 7.5, and 10 mM maltose buffer and used in EMSA experiments. A 247-bp fragment containing the two MYB binding sites of *ODO1* promoter ($ODO1_{fpro}$; Van Moerkercke et al., 2011) was PCR amplified using 5′ biotinylated or nonbiotinylated (used as competitor) primer set 29 (see Supplemental Table 1 online). To construct *EOBI* promoter target containing the potential consensus MYB binding sequence CTAACT (Sablowski et al., 1994), a 30-nucleotide long (biotinylated or not) oligonucleotide pair (5′-GACCTATATGTCTAACTTAATAGGTCTTTTCT-3′ and 5′-AGAAAAGACCTATTAAGTTAGACATATAGGTC-3′) corresponding to −1204 to −1174 bp upstream of the EOBI transcriptional start point was synthesized. Oligonucleotide pairs were heated to 80°C for 2 min and then cooled to room temperature (20°C) overnight. EMSA reactions were prepared according to the manufacturer's protocol (LightShift Chemiluminescent EMSA kit; Thermo Fisher Scientific) using binding buffer, 50 ng poly(dI-dC), proteins, competitor, noncompetitor, and biotin-labeled probes. The protein-probe mixture was separated in a native 6% polyacrylamide gel and transferred to a nylon membrane (Amersham). Migration of biotin-labeled probes was detected on x-ray film using streptavidin–horseradish peroxidase conjugates according to the manufacturer's protocol.

Y1H Analysis

To generate reporter strains, $ODO1_{fpro}$, IGS_{pro}, and PAL_{pro} promoter fragments were cloned into pENTR/D-TOPO (Invitrogen). In addition, a −764/−234

fragment from *ODO1* promoter was cloned as a negative control for the Y1H assay. Promoter fragments were then transferred to pGLacZi (Helfer et al., 2011) by LR recombination according to the manufacturer's protocol (Invitrogen) to generate $ODO1_{fpro}$:GLacZi, IGS_{pro}:GLacZi, and PAL_{pro}:GLacZi. pGLacZi derivatives were then integrated at the *URA3* site of *Saccharomyces cerevisiae* strain YM4271 (Clontech) by homologous recombination. To generate translational fusion of *EOBI* to the GAL4 activation domain (AD), the ORF of *EOBI* was amplified by PCR from $35S_{pro}$:EOBI and cloned into pENTR/D-TOPO, and LR was recombined into pDEST22 (Invitrogen) to generate pD22-EOBI. As a positive control, *EOBII* was cloned into pDEST22, generating pD22-EOBII. Yeast strain Y187 (Clontech) was transformed with an empty pDEST22 vector (pD22) as a negative control or with pD22-EOBI or pD22-EOBII. Reporter and activation strains were crossed, selected on medium lacking Trp and uracil, and tested for β-galactosidase activity by the colony-lift filter assay (Clontech).

Phylogenetic Analysis

The dendogram was constructed using the neighbor-joining algorithm with MEGA5 software (default settings; Tamura et al., 2011). Boostrapping was performed with 1000 replicates. A FASTA file of the ClustalW alignment used for dendogram construction is available as Supplemental Data Set 1 online.

Accession Numbers

Sequence data from this article can be found in GenBank/EMBL data libraries under the accession numbers listed in Supplemental Table 2 online.

Supplemental Data

The following materials are available in the online version of this article.

Supplemental Figure 1. Suppression of MYB-Related Sequences Affects Emission of Volatiles in Petunia Flowers.

Supplemental Figure 2. *EOBII* Overexpression in Petunia Flower Buds Leads to *EOBI* Upregulation.

Supplemental Figure 3. Confirmation of the Transgenic Origin of Independent Petunia Lines.

Supplemental Figure 4. EOBI Activates the Promoter and the Transcription of *IGS* in Petunia Leaves.

Supplemental Figure 5. Sequence Alignment of *Petunia hybrida* Line P720 *EOBI* and *EOBII*.

Supplemental Figure 6. Protein Sequence Alignment of EOBI Cloned from *Petunia hybrida* Lines P720 and W115.

Supplemental Table 1. List of Primers Used in This Study.

Supplemental Table 2. Accession Numbers of Genes and Proteins.

Supplemental Data Set 1. FASTA File of ClustalW Alignment Using MEGA5 Software.

ACKNOWLEDGMENTS

We thank the Danziger "Dan" Flower Farm for providing the plant material, Hillary Voet for assistance in the statistical analyses, and Emmanuel Koen, Sharona Shleizer-Burko, Yogev Burko, and Naomi Ori (The Hebrew University of Jerusalem, Israel) for the help with vector construction and Y1H. We thank Robert C. Schuurink (University of Amsterdam, The Netherlands) for kindly providing us with pBIN-$M19_{pro}$:GUS. This work was funded by Israel Science Foundation Grants 432/10, U.S.–Israel Binational Agricultural Research and Development Grant US-4322-10, and the Chief Scientist of the Israel Ministry of Agriculture and Rural Development. A.V. is an incumbent of the Wolfson Chair in Floriculture.

AUTHOR CONTRIBUTIONS

B.S.-R. designed and performed the research, analyzed the data, and wrote the article. B.A. and A.C. performed the research and analyzed the data. T.M., O.E., Y.Y., E.S., and M.O. performed the research. M.F. and M.M.B.Z. analyzed the data and wrote the article. A.V. designed the research and wrote the article.

Received September 16, 2012; revised November 26, 2012; accepted December 10, 2012; published December 28, 2012.

REFERENCES

Aharoni, A., De Vos, C.H.R., Wein, M., Sun, Z., Greco, R., Kroon, A., Mol, J.N.M., and O'Connell, A.P. (2001). The strawberry FaMYB1 transcription factor suppresses anthocyanin and flavonol accumulation in transgenic tobacco. Plant J. **28:** 319–332.

Aharoni, A., and Galili, G. (2011). Metabolic engineering of the plant primary-secondary metabolism interface. Curr. Opin. Biotechnol. **22:** 239–244.

Ben Zvi, M.M., Negre-Zakharov, F., Masci, T., Ovadis, M., Shklarman, E., Ben-Meir, H., Tzfira, T., Dudareva, N., and Vainstein, A. (2008). Interlinking showy traits: Co-engineering of scent and colour biosynthesis in flowers. Plant Biotechnol. J. **6:** 403–415.

Boatright, J., Negre, F., Chen, X., Kish, C.M., Wood, B., Peel, G., Orlova, I., Gang, D., Rhodes, D., and Dudareva, N. (2004). Understanding in vivo benzenoid metabolism in petunia petal tissue. Plant Physiol. **135:** 1993–2011.

Burow, M., Halkier, B.A., and Kliebenstein, D.J. (2010). Regulatory networks of glucosinolates shape *Arabidopsis thaliana* fitness. Curr. Opin. Plant Biol. **13:** 348–353.

Colquhoun, T.A., and Clark, D.G. (2011). Unraveling the regulation of floral fragrance biosynthesis. Plant Signal. Behav. **6:** 378–381.

Colquhoun, T.A., Kim, J.Y., Wedde, A.E., Levin, L.A., Schmitt, K.C., Schuurink, R.C., and Clark, D.G. (2011a). *PhMYB4* fine-tunes the floral volatile signature of *Petunia hybrida* through *PhC4H*. J. Exp. Bot. **62:** 1133–1143.

Colquhoun, T.A., Schwieterman, M.L., Wedde, A.E., Schimmel, B.C.J., Marciniak, D.M., Verdonk, J.C., Kim, J.Y., Oh, Y., Gális, I., Baldwin, I.T., and Clark, D.G. (2011b). EOBII controls flower opening by functioning as a general transcriptomic switch. Plant Physiol. **156:** 974–984.

Colquhoun, T.A., Verdonk, J.C., Schimmel, B.C.J., Tieman, D.M., Underwood, B.A., and Clark, D.G. (2010). Petunia floral volatile benzenoid/phenylpropanoid genes are regulated in a similar manner. Phytochemistry **71:** 158–167.

Croteau, R., and Karp, F. (1991). Origin of natural odorants. In Perfume: Art, Science and Technology, D. Lamparsky and M. Müller, eds (New York: Elsevier Applied Sciences), pp. 101–126.

Dal Cin, V., et al. (2011). Identification of genes in the phenylalanine metabolic pathway by ectopic expression of a MYB transcription factor in tomato fruit. Plant Cell **23:** 2738–2753.

Dare, A.P., Schaffer, R.J., Lin-Wang, K., Allan, A.C., and Hellens, R.P. (2008). Identification of a cis-regulatory element by transient analysis of co-ordinately regulated genes. Plant Methods **4:** 17.

Devaiah, B.N., Madhuvanthi, R., Karthikeyan, A.S., and Raghothama, K.G. (2009). Phosphate starvation responses and gibberellic acid

biosynthesis are regulated by the MYB62 transcription factor in *Arabidopsis*. Mol. Plant **2:** 43–58.

Dexter, R., Qualley, A., Kish, C.M., Ma, C.J., Koeduka, T., Nagegowda, D.A., Dudareva, N., Pichersky, E., and Clark, D. (2007). Characterization of a petunia acetyltransferase involved in the biosynthesis of the floral volatile isoeugenol. Plant J. **49:** 265–275.

Dias, A.P., Braun, E.L., McMullen, M.D., and Grotewold, E. (2003). Recently duplicated maize R2R3 Myb genes provide evidence for distinct mechanisms of evolutionary divergence after duplication. Plant Physiol. **131:** 610–620.

Dubos, C., Stracke, R., Grotewold, E., Weisshaar, B., Martin, C., and Lepiniec, L. (2010). MYB transcription factors in *Arabidopsis*. Trends Plant Sci. **15:** 573–581.

Dudareva, N., Pichersky, E., and Gershenzon, J. (2004). Biochemistry of plant volatiles. Plant Physiol. **135:** 1893–1902.

Farhi, M., Lavie, O., Masci, T., Hendel-Rahmanim, K., Weiss, D., Abeliovich, H., and Vainstein, A. (2010). Identification of rose phenylacetaldehyde synthase by functional complementation in yeast. Plant Mol. Biol. **72:** 235–245.

Feller, A., Machemer, K., Braun, E.L., and Grotewold, E. (2011). Evolutionary and comparative analysis of MYB and bHLH plant transcription factors. Plant J. **66:** 94–116.

Ferrer, J.L., Austin, M.B., and Stewart, C. Jr., and Noel, J.P. (2008). Structure and function of enzymes involved in the biosynthesis of phenylpropanoids. Plant Physiol. Biochem. **46:** 356–370.

Goodrich, K.R., and Raguso, R.A. (2009). The olfactory component of floral display in *Asimina* and *Deeringothamnus* (Annonaceae). New Phytol. **183:** 457–469.

Guo, Y., and Gan, S. (2011). AtMYB2 regulates whole plant senescence by inhibiting cytokinin-mediated branching at late stages of development in *Arabidopsis*. Plant Physiol. **156:** 1612–1619.

Guterman, I., Masci, T., Chen, X., Negre, F., Pichersky, E., Dudareva, N., Weiss, D., and Vainstein, A. (2006). Generation of phenylpropanoid pathway-derived volatiles in transgenic plants: Rose alcohol acetyltransferase produces phenylethyl acetate and benzyl acetate in petunia flowers. Plant Mol. Biol. **60:** 555–563.

Helfer, A., Nusinow, D.A., Chow, B.Y., Gehrke, A.R., Bulyk, M.L., and Kay, S.A. (2011). *LUX ARRHYTHMO* encodes a nighttime repressor of circadian gene expression in the *Arabidopsis* core clock. Curr. Biol. **21:** 126–133.

Hippauf, F., Michalsky, E., Huang, R., Preissner, R., Barkman, T.J., and Piechulla, B. (2010). Enzymatic, expression and structural divergences among carboxyl O-methyltransferases after gene duplication and speciation in *Nicotiana*. Plant Mol. Biol. **72:** 311–330.

Hoballah, M.E., Stuurman, J., Turlings, T.C., Guerin, P.M., Connétable, S., and Kuhlemeier, C. (2005). The composition and timing of flower odour emission by wild *Petunia axillaris* coincide with the antennal perception and nocturnal activity of the pollinator *Manduca sexta*. Planta **222:** 141–150.

Horiuchi, J., Badri, D.V., Kimball, B.A., Negre, F., Dudareva, N., Paschke, M.W., and Vivanco, J.M. (2007). The floral volatile, methyl benzoate, from snapdragon (*Antirrhinum majus*) triggers phytotoxic effects in *Arabidopsis thaliana*. Planta **226:** 1–10.

Jin, H., Cominelli, E., Bailey, P., Parr, A., Mehrtens, F., Jones, J., Tonelli, C., Weisshaar, B., and Martin, C. (2000). Transcriptional repression by AtMYB4 controls production of UV-protecting sunscreens in *Arabidopsis*. EMBO J. **19:** 6150–6161.

Jin, H., and Martin, C. (1999). Multifunctionality and diversity within the plant MYB-gene family. Plant Mol. Biol. **41:** 577–585.

Kaminaga, Y., et al. (2006). Plant phenylacetaldehyde synthase is a bifunctional homotetrameric enzyme that catalyzes phenylalanine decarboxylation and oxidation. J. Biol. Chem. **281:** 23357–23366.

Kang, Y.H., Kirik, V., Hulskamp, M., Nam, K.H., Hagely, K., Lee, M.M., and Schiefelbein, J. (2009). The MYB23 gene provides a positive feedback loop for cell fate specification in the *Arabidopsis* root epidermis. Plant Cell **21:** 1080–1094.

Karlova, R., Rosin, F.M., Busscher-Lange, J., Parapunova, V., Do, P.T., Fernie, A.R., Fraser, P.D., Baxter, C., Angenent, G.C., and de Maagd, R.A. (2011). Transcriptome and metabolite profiling show that APETALA2a is a major regulator of tomato fruit ripening. Plant Cell **23:** 923–941.

Kaufmann, K., Pajoro, A., and Angenent, G.C. (2010). Regulation of transcription in plants: Mechanisms controlling developmental switches. Nat. Rev. Genet. **11:** 830–842.

Klahre, U., Gurba, A., Hermann, K., Saxenhofer, M., Bossolini, E., Guerin, P.M., and Kuhlemeier, C. (2011). Pollinator choice in Petunia depends on two major genetic loci for floral scent production. Curr. Biol. **21:** 730–739.

Klempien, A., et al. (2012). Contribution of CoA ligases to benzenoid biosynthesis in petunia flowers. Plant Cell **24:** 2015–2030.

Knudsen, J.T., Eriksson, R., Gershenzon, J., and Stahl, B. (2006). Diversity and distribution of floral scent. Bot. Rev. **72:** 1–120.

Koeduka, T., Louie, G.V., Orlova, I., Kish, C.M., Ibdah, M., Wilkerson, C.G., Bowman, M.E., Baiga, T.J., Noel, J.P., Dudareva, N., and Pichersky, E. (2008). The multiple phenylpropene synthases in both *Clarkia breweri* and *Petunia hybrida* represent two distinct protein lineages. Plant J. **54:** 362–374.

Koes, R., Verweij, W., and Quattrocchio, F. (2005). Flavonoids: A colorful model for the regulation and evolution of biochemical pathways. Trends Plant Sci. **10:** 236–242.

Kolosova, N., Gorenstein, N., Kish, C.M., and Dudareva, N. (2001). Regulation of circadian methyl benzoate emission in diurnally and nocturnally emitting plants. Plant Cell **13:** 2333–2347.

Kranz, H.D., et al. (1998). Towards functional characterisation of the members of the R2R3-MYB gene family from *Arabidopsis thaliana*. Plant J. **16:** 263–276.

Leitner-Dagan, Y., Ovadis, M., Shklarman, E., Elad, Y., Rav David, D., and Vainstein, A. (2006). Expression and functional analyses of the plastid lipid-associated protein CHRC suggest its role in chromoplastogenesis and stress. Plant Physiol. **142:** 233–244.

Li, J.G., Yang, X.Y., Wang, Y., Li, X.J., Gao, Z.F., Pei, M., Chen, Z.L., Qu, L.J., and Gu, H.Y. (2006). Two groups of MYB transcription factors share a motif which enhances trans-activation activity. Biochem. Biophys. Res. Commun. **341:** 1155–1163.

Liu, Y., Schiff, M., and Dinesh-Kumar, S.P. (2002). Virus-induced gene silencing in tomato. Plant J. **31:** 777–786.

Locatelli, F., Vannini, C., Magnani, E., Coraggio, I., and Bracale, M. (2003). Efficiency of transient transformation in tobacco protoplasts is independent of plasmid amount. Plant Cell Rep. **21:** 865–871.

Long, M.C., Nagegowda, D.A., Kaminaga, Y., Ho, K.K., Kish, C.M., Schnepp, J., Sherman, D., Weiner, H., Rhodes, D., and Dudareva, N. (2009). Involvement of snapdragon benzaldehyde dehydrogenase in benzoic acid biosynthesis. Plant J. **59:** 256–265.

Maeda, H., Shasany, A.K., Schnepp, J., Orlova, I., Taguchi, G., Cooper, B.R., Rhodes, D., Pichersky, E., and Dudareva, N. (2010). RNAi suppression of *Arogenate Dehydratase1* reveals that phenylalanine is synthesized predominantly via the arogenate pathway in petunia petals. Plant Cell **22:** 832–849.

Maeda, H., Yoo, H., and Dudareva, N. (2011). Prephenate aminotransferase directs plant phenylalanine biosynthesis via arogenate. Nat. Chem. Biol. **7:** 19–21.

Malitsky, S., Blum, E., Less, H., Venger, I., Elbaz, M., Morin, S., Eshed, Y., and Aharoni, A. (2008). The transcript and metabolite networks affected by the two clades of *Arabidopsis* glucosinolate biosynthesis regulators. Plant Physiol. **148:** 2021–2049.

Mandaokar, A., and Browse, J. (2009). MYB108 acts together with MYB24 to regulate jasmonate-mediated stamen maturation in *Arabidopsis*. Plant Physiol. **149:** 851–862.

Moyano, E., Martínez-Garcia, J.F., and Martin, C. (1996). Apparent redundancy in *myb* gene function provides gearing for the control of flavonoid biosynthesis in *Antirrhinum* flowers. Plant Cell **8:** 1519–1532.

Nakai, K., and Horton, P. (1999). PSORT: A program for detecting sorting signals in proteins and predicting their subcellular localization. Trends Biochem. Sci. **24:** 34–36.

Pichersky, E., and Lewinsohn, E. (2011). Convergent evolution in plant specialized metabolism. Annu. Rev. Plant Biol. **62:** 549–566.

Preston, J., Wheeler, J., Heazlewood, J., Li, S.F., and Parish, R.W. (2004). AtMYB32 is required for normal pollen development in *Arabidopsis thaliana*. Plant J. **40:** 979–995.

Quattrocchio, F., Verweij, W., Kroon, A., Spelt, C., Mol, J., and Koes, R. (2006). PH4 of *Petunia* is an R2R3 MYB protein that activates vacuolar acidification through interactions with basic-helix-loop-helix transcription factors of the anthocyanin pathway. Plant Cell **18:** 1274–1291.

Sablowski, R.W.M., Moyano, E., Culianez-Macia, F.A., Schuch, W., Martin, C., and Bevan, M. (1994). A flower-specific Myb protein activates transcription of phenylpropanoid biosynthetic genes. EMBO J. **13:** 128–137.

Schwachtje, J., and Baldwin, I.T. (2008). Why does herbivore attack reconfigure primary metabolism? Plant Physiol. **146:** 845–851.

Schwinn, K., Venail, J., Shang, Y.J., Mackay, S., Alm, V., Butelli, E., Oyama, R., Bailey, P., Davies, K., and Martin, C. (2006). A small family of *MYB*-regulatory genes controls floral pigmentation intensity and patterning in the genus *Antirrhinum*. Plant Cell **18:** 831–851.

Shin, B., Choi, G., Yi, H., Yang, S., Cho, I., Kim, J., Lee, S., Paek, N.-C., Kim, J.-H., Song, P.-S., and Choi, G. (2002). *AtMYB21*, a gene encoding a flower-specific transcription factor, is regulated by COP1. Plant J. **30:** 23–32.

Sønderby, I.E., Burow, M., Rowe, H.C., Kliebenstein, D.J., and Halkier, B.A. (2010). A complex interplay of three R2R3 MYB transcription factors determines the profile of aliphatic glucosinolates in *Arabidopsis*. Plant Physiol. **153:** 348–363.

Spelt, C., Quattrocchio, F., Mol, J.N.M., and Koes, R. (2000). *anthocyanin1* of petunia encodes a basic helix-loop-helix protein that directly activates transcription of structural anthocyanin genes. Plant Cell **12:** 1619–1632.

Spitzer, B., et al. (2007). Reverse genetics of floral scent: Application of tobacco rattle virus-based gene silencing in Petunia. Plant Physiol. **145:** 1241–1250.

Spitzer-Rimon, B., Marhevka, E., Barkai, O., Marton, I., Edelbaum, O., Masci, T., Prathapani, N.-K., Shklarman, E., Ovadis, M., and Vainstein, A. (2010). EOBII, a gene encoding a flower-specific regulator of phenylpropanoid volatiles' biosynthesis in petunia. Plant Cell **22:** 1961–1976.

Stafford, H.A. (1991). Flavonoid evolution: An enzymic approach. Plant Physiol. **96:** 680–685.

Tamagnone, L., Merida, A., Parr, A., Mackay, S., Culianez-Macia, F.A., Roberts, K., and Martin, C. (1998). The AmMYB308 and AmMYB330 transcription factors from *Antirrhinum* regulate phenylpropanoid and lignin biosynthesis in transgenic tobacco. Plant Cell **10:** 135–154.

Tamura, K., Peterson, D., Peterson, N., Stecher, G., Nei, M., and Kumar, S. (2011). MEGA5: Molecular evolutionary genetics analysis using maximum likelihood, evolutionary distance, and maximum parsimony methods. Mol. Biol. Evol. **28:** 2731–2739.

Tieman, D., Taylor, M., Schauer, N., Fernie, A.R., Hanson, A.D., and Klee, H.J. (2006). Tomato aromatic amino acid decarboxylases participate in synthesis of the flavor volatiles 2-phenylethanol and 2-phenylacetaldehyde. Proc. Natl. Acad. Sci. USA **103:** 8287–8292.

Toledo-Ortiz, G., Huq, E., and Rodríguez-Concepción, M. (2010). Direct regulation of phytoene synthase gene expression and carotenoid biosynthesis by phytochrome-interacting factors. Proc. Natl. Acad. Sci. USA **107:** 11626–11631.

Tzfira, T., Tian, G.-W., Lacroix, B.T., Vyas, S., Li, J., Leitner-Dagan, Y., Krichevsky, A., Taylor, T., Vainstein, A., and Citovsky, V. (2005). pSAT vectors: A modular series of plasmids for autofluorescent protein tagging and expression of multiple genes in plants. Plant Mol. Biol. **57:** 503–516.

Uimari, A., and Strommer, J. (1997). Myb26: A MYB-like protein of pea flowers with affinity for promoters of phenylpropanoid genes. Plant J. **12:** 1273–1284.

van der Fits, L., and Memelink, J. (2000). ORCA3, a jasmonate-responsive transcriptional regulator of plant primary and secondary metabolism. Science **289:** 295–297.

Van Moerkercke, A., Haring, M.A., and Schuurink, R.C. (2011). The transcription factor EMISSION OF BENZENOIDS II activates the MYB *ODORANT1* promoter at a MYB binding site specific for fragrant petunias. Plant J. **67:** 917–928.

Van Moerkercke, A., Schauvinhold, I., Pichersky, E., Haring, M.A., and Schuurink, R.C. (2009). A plant thiolase involved in benzoic acid biosynthesis and volatile benzenoid production. Plant J. **60:** 292–302.

Verdonk, J.C., Haring, M.A., van Tunen, A.J., and Schuurink, R.C. (2005). ODORANT1 regulates fragrance biosynthesis in petunia flowers. Plant Cell **17:** 1612–1624.

Vogt, T. (2010). Phenylpropanoid biosynthesis. Mol. Plant **3:** 2–20.

Wilkins, O., Nahal, H., Foong, J., Provart, N.J., and Campbell, M.M. (2009). Expansion and diversification of the Populus R2R3-MYB family of transcription factors. Plant Physiol. **149:** 981–993.

Zhang, P., Chopra, S., and Peterson, T. (2000). A segmental gene duplication generated differentially expressed myb-homologous genes in maize. Plant Cell **12:** 2311–2322.

Zhong, R., Lee, C., and Ye, Z.H. (2010). Evolutionary conservation of the transcriptional network regulating secondary cell wall biosynthesis. Trends Plant Sci. **15:** 625–632.

Zvi, M.M., Shklarman, E., Masci, T., Kalev, H., Debener, T., Shafir, S., Ovadis, M., and Vainstein, A. (2012). PAP1 transcription factor enhances production of phenylpropanoid and terpenoid scent compounds in rose flowers. New Phytol. **195:** 335–345.